DEPARTMENT OF PHYSICS, UNIVERSITY OF JYVÄSKYLÄ
RESEARCH REPORT No. 3/1979

E0 AND E2 DECAY OF LOW-LYING 0^+ STATES IN THE EVEN-EVEN NUCLEI ^{206}Pb, ^{208}Po, $^{112-120}$Sn AND $^{112,\,114}$Cd

BY

RAUNO JULIN

Academic dissertation
for the Degree of
Doctor of Philosophy

Jyväskylä Finland
April 1979

ISBN 951-678-152-7

URN:ISBN:978-951-39-9454-9
ISBN 978-951-39-9454-9 (PDF)
ISSN 0075-465X

Jyväskylän yliopisto, 2022

ISBN 951-678-152-7
ISSN 0075-465X

DEPARTMENT OF PHYSICS, UNIVERSITY OF JYVÄSKYLÄ
RESEARCH REPORT No. 3/1979

E0 AND E2 DECAY OF LOW-LYING 0^+ STATES IN THE EVEN-EVEN NUCLEI ^{206}Pb, ^{208}Po, $^{112-120}$Sn AND ^{112,114}Cd

BY

RAUNO JULIN

Academic dissertation
for the Degree of
Doctor of Philosophy

To be presented, by permission ot the
Faculty of Mathematics and Natural Sciences
of the University of Jyväskylä
for public examination in Auditorium II-212 of the
University on May 9, 1979, at 12 o'clock noon.

Jyväskylä Finland
April 1979

Preface

This work has been carried out during the years 1975 - 1978 at the Department of Physics, University of Jyväskylä, Finland, and at the Tandem Accelerator Laboratory, University of Uppsala, Sweden. I wish to express my thanks to these institutes for the excellent working conditions provided for me.

It is a pleasure for me to express my sincere gratitude to my teacher, Professor J. Kantele. He has initiated the EO project and offered a wealth of ideas, continuous encouragement and support throughout the course of this work.

To my coworkers, Dr. A. Bäcklin; Mr. N.-G. Jonsson, M.Sc.; Mr. M. Luontama, M.Sc.; Mr. A. Passoja, Lic. Phil. and Mr. T. Poikolainen, M.Sc., I am greatly indebted for enjoyable co-operation. I also want to extend my thanks to the staffs of the cyclotron, the computer, the target laboratory and the machine shops at JYFL for their valuable assistance and co-operation. I wish to thank all my other colleagues, as well.

I am indebted to Professor P.O. Lipas for revising the language of the manuscript. My thanks also go to Mrs. M. Selosmaa and to Miss P. Pitkänen, who carefully typed this thesis and to Mr. T. Näränen, who skillfully finished the drawings.

This work has been financially supported by grants from the Emil Aaltonen Foundation, the Oskar Öflund Foundation, the Ellen and Artturi Nyyssönen Foundation and by travel grants from the Nordic Comitée for Accelerator Based Research. This aid is gratefully acknowledged.

To my wife and my daughters I owe a great depth of gratitude for their support and understanding.

Jyväskylä, March 1979

Rauno Julin

E0 AND E2 DECAY OF LOW-LYING 0^+ STATES IN THE EVEN-EVEN NUCLEI ^{206}Pb, ^{208}Po, $^{112-120}Sn$ AND $^{112,114}Cd$

Abstract

Several new methods of in-beam conversion-electron and γ-ray spectrometry, applicable in the determination of E0 and E2 decay properties of low-lying 0^+ states in even-mass nuclei, have been developed. The main attention has been paid to direct lifetime-measurement and coincidence methods based on the use of the natural pulsing of a cyclotron beam. With the aid of these methods, the similarity of the absolute decay rates of the two-neutron-hole 0_2^+ states in the N = 124 nuclei ^{206}Pb and ^{208}Po has been shown. A systematic investigation of the de-excitation of the 0_2^+ and 0_3^+ states in $^{112,114,116,118,120}Sn$ has been carried out: twelve E0 transitions connecting the 0^+ states have been observed, including very strong low-energy E0 transitions between the excited 0^+ states, and several absolute transition probabilities have been determined. Furthermore, the new techniques have been applied successfully in determining the absolute E0 and E2 transition rates from the 0_2^+ and 0_3^+ states in ^{112}Cd and ^{114}Cd. The use of isotope-shift data in the calculation of the monopole strengths in ^{206}Pb and ^{208}Po is discussed. The results on even Sn and Cd nuclei are discussed within the framework of the coexistence of different shapes and of configuration mixing.

Contents

1. INTRODUCTION

Even-even nuclei exhibit in general at least one 0^+ state at low excitation energies ($\leq$ 2 MeV). In several nuclei two or sometimes even five such states are among the very lowest excited states[1]. At present, there is no exact theoretical description of most of these states and thus the experimental study of the properties of these levels is of special importance.

The most valuable systematic data for studies of the structure of 0^+ states have been obtained from various transfer reactions in which the 0^+ excitations are the subject of a growing interest. Experimental data on the characteristics of electric monopole (E0; $0^+ \rightarrow 0^+$) and electric quadrupole (E2; $0^+ \rightarrow 2^+$) transitions from the excited 0^+ states have been scarce.

Electric monopole transitions proceed by internal conversion, and for energies greater than 2 $m_e c^2$ also by pair production. The contribution of internal conversion increases with atomic number and with decreasing transition energy so that for E0 transitions of < 2 MeV in nuclei with mass number $A > 100$ it is dominating. An E0 conversion is a penetration effect where the transition is caused by a Coulomb interaction between nuclear protons and atomic shell electrons penetrating inside the nucleus[2].

The E0 transition probability can be written as[2]

$$W_i(E0) = \Omega_i \rho^2,$$

where Ω_i is an electronic factor which is a known function for a given electron shell i. The monopole strength parameter ρ for an

$E0(0_i^+ \rightarrow 0_f^+)$ transition is defined as

$$\rho = \langle 0_f^+ | \sum_j e_j r_j^2 | 0_i^+ \rangle / eR^2,$$

where R is the nuclear radius ($1.2\ A^{1/3}$fm) and where the monopole operator in the monopole matrix element is taken as a sum over the charged particles in the nucleus. Accordingly the ρ^2 value is related to the reduced E0 transition probability B(E0), which is the square of the monopole matrix element. If the absolute transition probabilities cannot be determined, the experimental ratio of reduced transition probabilities of the competing E0 and E2 transitions de-exciting the 0^+ state is reported:

$$X = \frac{B(E0)}{B(E2)} = \frac{e^2\rho^2R^4}{B(E2)} .$$

The monopole matrix element is determined exclusively by the wave functions of the 0^+ states, and thus an investigation of the monopole transitions provides information on the nature of these states.

Experimental data on the energies and decay properties of the excited 0^+ states in even-even nuclei have been collected and systematized in ref. 1. In cases where an E0 conversion is observed, typically only the X value is reported. Systematic studies are scarce and the absolute ρ value is usually known only in the cases where the corresponding 0^+ state can be reached in Coulomb excitation. Direct lifetime measurements of 0^+states have been performed only in some very favourable cases. The need for additional experimental data on the decay of the 0^+ states has been recognized for a long time[3,4].

Although there is no good theoretical explanation for the existence

of most of the low-energy 0^+ states, a variety of theoretical descriptions can be found. In the simple shell-model picture of 0^+ states, the excited 0^+ state and the ground state are pair-correlated states, the excited 0^+ state being orthogonal to the ground state, which is a configuration mixing of two-particle shell-model states[5]. This interpretation is sometimes applicable in nuclei near the closed neutron or proton shells.

The first excited 0^+ level (0_2^+) in spherical vibrational nuclei is often characterized as a collective two-phonon state which in deformed nuclei correspondingly is a β-vibrational 0^+ state. An enhanced E2 transition to the 2_1^+ state and a relatively large ρ value associated with the E0 transition to the ground state are characteristic of the decay of this 0^+ state.

Excited pairing-vibrational 0^+ states[6] which are populated in two-nucleon transfer reactions should generally be observed at relatively high excitation energy. However, various disturbing effects sometimes make low-energy pairing-vibrational excitations possible. Particularly interesting are very recent results[7] on proton pairing-vibrational states, which e.g. in even mass Sn nuclei give a new alternative description of the collective 0_2^+ states.

A nonenhanced E2 transition to the 2_1^+ state is often characteristic of the decay of the low-lying 0^+ states which cannot be related to the two-phonon states. In the theoretical explanation of the existence of these states a wide variety of interactions are called for. In the collective picture one of these states is a vibrational excitation of a nonaxially deformed nucleus[8] or a three-phonon state, which is pushed down due to the γ softness of the nucleus[9].

The shortage of experimental data on the decay of the 0^+ states is understandable when considering the fact that in detecting E0 transitions and particularly in determining absolute transition probabilities several methods of nuclear spectroscopy have to be available. The main body of the present information has been obtained in off-line conversion-electron measurements utilizing the β decay of nuclei in the excitation of the 0^+ states. Clearly, in-beam measurements are required for obtaining systematic information. Different kinds of methods of in-beam conversion-electron and gamma-ray spectroscopy are needed, and methods for direct in-beam lifetime measurements have to be developed. Furthermore, in the investigation of the collective 0^+ states , methods of Coulomb excitation are also needed.

The study of the decay of the 0^+ states is a suitable project in a laboratory like the Department of Physics, University of Jyväskylä, where a 90 cm cyclotron can be employed. For this project different types of in-beam electron spectrometers, especially a spectrometer suited to electron - heavy-particle coincidence measurements, have been constructed[10,11]. For the lifetime determination of the 0^+ states, direct lifetime measurement methods based on the use of the pulsed beam of the cyclotron have been developed[12,13].

Particularly in the study of 0^+ states in Sn nuclei the use of several methods has been possible through the joint effort of groups at the Department of Physics, University of Jyväskylä, and the Institute of Physics and Tandem Accelerator Laboratory, University of Uppsala, Sweden. The heavy ion beams from the Uppsala EN Tandem have been

employed in the Coulomb excitation studies, and in cases where a 0^+ state is populated through an isobaric analog resonance (IAR), the proton beam of well-defined energy from the Tandem is useful.

This work is a part of the above-mentioned project, and here decay properties of low-energy 0^+ states in the even-even nuclei ^{206}Pb, ^{208}Po, $^{112,114,116,118,120}Sn$ and $^{112,114}Cd$ have been investigated. A considerable part of this thesis consists of the presentation of the experimental methods employed. Most attention has been paid to new direct lifetime-measurement methods based on the use of the natural pulsing of the cyclotron beam. Most of the experimental methods and results presented in this thesis have been included in the following papers:

List of included articles

1. J. Kantele, M. Luontama, A. Passoja and R. Julin:
   A swept-current magnetic lens plus Si(Li) electron spectrometer with simultaneous momentum and energy selection
   Nucl. Instr. and Meth. 130 (1975) 467
   https://doi.org/10.1016/0029-$_{SS}$4X(7$_S$)90044-0
2. R. Julin, J. Kantele, M. Luontama, T. Poikolainen and V. Rahkonen:
   Half-lives of the two-neutron-hole 0_2^+ states in ^{206}Pb and ^{208}Po
   Phys. Lett. 65B (1976) 337
   https://doi.org/10.1016/0370-2693(76)90236-7
3. R. Julin, J. Kantele, M. Luontama, A. Passoja and T. Poikolainen:
   A walk-free centroid method for lifetime measurements with pulsed beams
   Nucl. Instr. and Meth. 152 (1978) 471
   https://doi.org/10.1016/0029-$_{SS}$4X(78)90048-4

4. J. Kantele, R. Julin, M. Luontama, A. Passoja, T. Poikolainen, A. Bäcklin and N.-G. Jonsson:
Absolute E0 and E2 transition rates and collective states in ^{116}Sn
Z. Physik 289 (1979) 157
https://doi.org/10.1007/BF01435933

5. M. Luontama, J. Kantele, R. Julin, A. Passoja, T. Poikolainen and M. Pylvänäinen:
A combination intermediate-image magnetic plus Si(Li) electron spectrometer for in-beam experiments
Nucl. Instr. and Meth., 159 (1979) 339
https://doi.org/10.1016/0029-554X(79)90659-1

6. A. Bäcklin, N.-G. Jonsson, R. Julin, J. Kantele, M. Luontama, A. Passoja and T. Poikolainen:
0^+ states and absolute E0 and E2 transition rates in even Sn nuclei, to be published
https://doi.org/10.1016/0375-9474(81)90184-6

2. EXPERIMENTAL METHODS

In practice, the goal in the investigation of the decay of a 0^+ state is to determine the lifetime of this state and to measure the branching ratio of the de-exciting E2 and E0 transitions. Since low-energy E0 transitions mainly proceed by internal conversion, the branching ratios can in favourable cases be obtained in the singles conversion-electron spectrum. However, for a firm identification of an E2 transition and for showing the absence of a gamma line corresponding to an E0 transition, the gamma-ray spectrum is always needed. Typically, the identification of an E0 conversion-electron line in the high-energy part of the electron spectrum is easy because of the weakness of internal conversion of other high-energy transitions. On the contrary, the identification of peaks corresponding to lower-energy E2 transitions and to E0 transitions between the excited 0^+ states in the complex part of the electron spectrum, especially in in-beam measurements, is usually more difficult. For this reason, the reactions (d,p) and (p,p'), which allow proton-electron and proton-gamma coincidence measurements, are very important in the excitation of 0^+ states. An electron spectrometer adapted to proton-electron coincidence measurements is presented in subsect. 2.2.2.

Lifetime-measurement methods based on the detection of E0 conversion electrons and on the use of a pulsed beam are presented in subsects. 2.3.2 and 2.3.3. In subsect. 2.3.4 a walk-free centroid method based on the proton-gamma coincidence measurement and on the use of a pulsed beam is presented. This method can be

applied when a 0^+ state is populated in the (d,p) or (p,p') reactions and the level density of the final nucleus is sufficiently low. In this work double Coulomb excitation has also been applied to the determination of transition probabilities.

2.1. Gamma-ray spectrometry

In the measurements of gamma-ray spectra, several coaxial Ge(Li) detectors with active volumes ranging from 40 cm^3 to 120 cm^3, a 7 cm^3 planar intrinsic germanium detector and a 0.5 cm^3 LEPS-germanium detector were employed. The energy resolution was typically 2.0-2.5 keV at 1 MeV for the coaxial detectors, 700 eV at 120 keV and about 1.7 keV at 1 MeV for the 7 cm^3 detector, and about 600 eV at 120 keV for the LEPS detector.

In gamma-proton coincidence measurements, two types of detector set-up were used. In the investigation of the decay of the 0_3^+ state in ^{112}Cd, where the 0_3^+ level was populated in the $^{111}Cd(d,p)^{112}Cd$ reaction, a 300 mm^2x100 μm silicon surface-barrier detector (Si(Au)), positioned at about 2 cm from the target, at 90° to the beam direction, was used. Deuterons scattered from the target were absorbed by means of a 0.5 mm thick aluminium absorber in front of the Si(Au) detector. The 7 cm^3 planar germanium detector was used for gamma-ray detection. In the investigation of 0^+ states in even Sn nuclei, a gamma-proton coincidence set-up was used to find the population of 0^+ and other low-spin states in proton inelastic scattering. In this set-up scattered protons were detected with a 2 cm^2, 1.5 mm thick annular Si(Au) detector placed

at 180° to the beam. A single-channel analyzer was used to select scattered protons corresponding to excitation energies of about 1 to 5 MeV. The γ-ray detector was a 120 cm^3 Ge(Li) crystal placed at 90° to the beam.

2.2. Conversion-electron spectrometry

2.2.1. Electron spectrometers

Three types of magnetic lens plus Si(Li) combination in-beam electron spectrometers[10,11,14] were employed in this work. These spectrometers can be used in a fixed- or swept-current mode of operation. In the fixed-current mode a certain energy region is selected, in which case the width of the energy region is determined by the momentum band-width $\frac{\Delta p}{p}$ of the lens, and the total efficiency is determined by the transmission of the spectrometer and the efficiency of the Si(Li) detector[10]. In the swept-current mode a large energy region is investigated and in this mode of operation a sweeping-mode efficiency has to be considered[10]. A background reduction system based on a simultaneous momentum and energy selection is in operation with all of these spectrometers. The background due to β^+ activities is removed with the aid of anti-positron baffles.

In Uppsala a ring-focus magnetic lens spectrometer with a 2 mm thick, 200 mm^2 or 500 mm^2 Kevex Si(Li) detector with cooled FET pre-amplifier was used[14]. The transmission of this spectrometer is 1.2 % for the 200 mm^2 detector and 1.7 % for the 500 mm^2 detector, and an

energy resolution of 2.0 keV and 2.3 keV, respectively, at 1 MeV can be achieved. This spectrometer was employed in obtaining singles electron spectra in the study of Sn nuclei.

In Jyväskylä two types of electron spectrometer have been designed. The first one[10] is somewhat similar to that used in Uppsala, and it was used in this work primarily in direct lifetime measurements with a small scintillation detector in place of the Si(Li) detector (fig. 4). The second one is a magnetic lens plus Si(Li) arrangement shown in fig. 1, which has focusing properties and a field shape similar to those of an intermediate-image spectrometer.

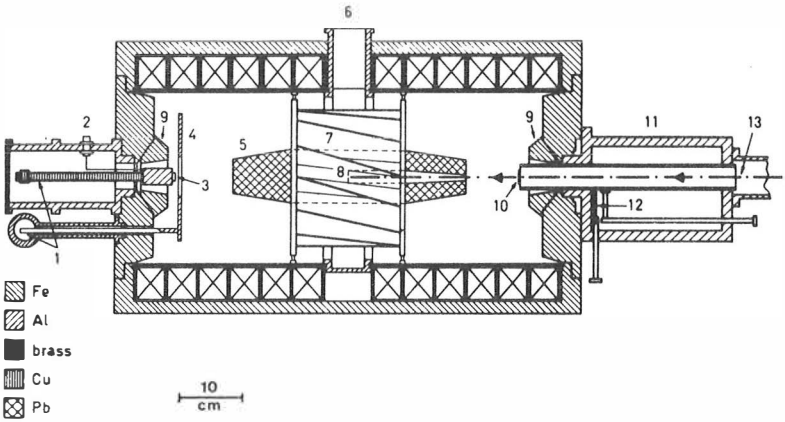

Fig. 1. Schematic cross-sectional diagram of the combined intermediate-image magnetic + Si(Li) electron spectrometer configuration: (1) cold fingers, (2) to preamplifier, (3) Si(Li) electron detector, (4) cold trap, (5) lead shield, (6) to pump, (7) anti-positron baffle, (8) Faraday cup, (9) extra iron pieces, (10) target/source, (11) target/source changing system, (12) gate valve, (13) beam (collimators not shown)

A transmission up to 7 % and a momentum bancwidth of 24 % are achieved by placing both the target and the detector in a high magnetic field inside the lens. The electron acceptance angle of this spectrometer is about 50°, which corresponds to $P_2(\cos\theta) \sim P_2(\cos 55^{o}) = 0$. For that reason problems associated with angular distributions and particle parameters are diminished. A 110 mm^2 by 3 mm thick Kevex Si(Li) detector and an 80 mm^2 by 2 mm thick Kevex Si(Li) detector with a cooled FET preamplifier were used with this spectrometer. The energy resolution of the 110 mm^2 Si(Li) detector is about 2.5 keV at 1 MeV. With the 80 mm^2 Si(Li) detector, resolutions of about 1.4 keV at 300 keV and about 2 keV at 1 MeV can be achieved. In a typical in-beam run the target thickness limits the resolution to about 3 keV.

The energy calibration of the electron spectrometers was done by means of internal calibration or with ^{133}Ba, ^{207}Bi and ^{152}Eu sources.

The determination of the peak-to-total ratio (PTR) curve for the efficiency curve[10)] of the electron spectrometers was carried out with the aid of the former sources or sources of continuous electron spectra. The relative efficiency curves obtained are believed to be accurate to better than ± 10 %.

2.2.2. Electron - heavy-particle coincidence arrangement

The geometry and the high transmission of the combination intermediate-image magnetic plus Si(Li) electron spectrometer construction described above allow the use of this spectrometer in electron - heavy-

particle coincidence experiments. These measurements are carried out by placing an annular Si(Au) detector near the target, at back angles, as sketched in fig. 2. The cyclotron beam is focused and steered through the hole in the annular detector. The diameter of the detector is 1.6 cm, the thickness 1.5 mm, the active area 160 mm^2 and the hole diameter 6 mm. The solid angle of detection for the set-up in fig. 2 is approximately 10 % of 4π. The backscattering of the beam particles from the Faraday cup (fig. 1) is strongly reduced by the use of a narrow hole (ϕ = 8 mm) at the entrance to the Faraday cup.

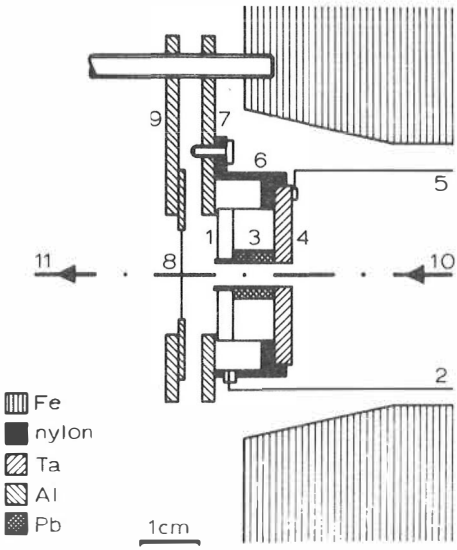

Fig. 2. Cross-sectional diagram of the target and the coincidence detector set-up: (1) coincidence detector, (2) to preamplifier, (3) lead collimator, (4) tantalum collimator, (5) to charge integrator, (6) nylon case, (7) aluminium detector holder, (8) target, (9) aluminium target holder, (10) beam, (11) to Faraday cup

ARC timing techniques are used in deriving the information from both the Si(Li) electron detector and the Si(Au) particle detector, and the coincidence-timing window width is chosen to be about 20 ns. False coincidences caused by beam particles scattered from the Faraday cup are eliminated by imposing an additional condition to ensure that the time delay between the Si(Au) detector pulse and the cyclotron beam pulse corresponds to the scattering of the particle from the target. The energy information from both detectors is usually fed through a CAMAC interface to a PDP-11/45 computer. The CAMAC gate pulse represents the fulfillment of the coincidence and other conditions. The data are collected event by event on a magnetic tape for a subsequent analysis.

In this work the coincidence set-up has been used successfully in conjunction with the reactions (p,p') and (d,p). Fig. 3 shows parts of conversion electron spectra obtained in coincidence with protons inelastically scattered from a 0.5 mg/cm^2 thick ^{116}Sn target. The E0 transition between the excited 0^+ states ($0_3^+ \rightarrow 0_2^+$) and the competing E2 transition ($0_3^+ \rightarrow 2_i^+$) can be seen in these spectra obtained with fixed current settings in the lens. In this case the excitation cross section of the 0_3^+ state was only about 30 μb/st at backward angles. The proton energy resolution, of the order of 100 keV, of the annular Si(Au) detector allowed the placing of an energy window in the proton spectrum which was used in the level selection and in the reduction of the background due to the (p,xn) reactions and to activities built up in the target. In the case of the (p,p') reaction, an upper limit for the usable beam current is set by the maximum allowable counting rate of the heavy-particle detector. In the present measurements, this

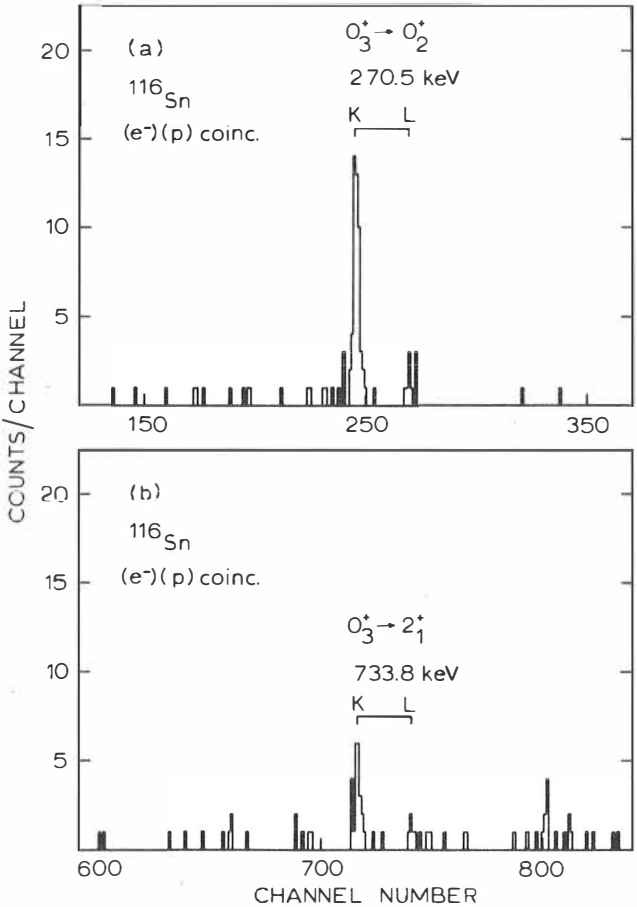

Fig. 3. Parts of conversion-electron spectra obtained in coincidence with protons inelastically scattered from a 0.5 mg/cm^2 thick ^{116}Sn target. The bombarding energy was 7.9 MeV, and the gating window in the proton spectrum was placed on the peak corresponding to the scattering from the 0_3^+ level at 2027 keV in ^{116}Sn. The recording times were a) 2 h, b) 18 h.

was about 2 to 4 x 10^4 cps, predominantly caused by particles elastically scattered from the target.

The coincidence arrangement in conjunction with the (d,p) reaction was used in a study of the decay of the 0_3^+ state in ^{112}Cd (fig. 16). In this case an aluminium absorber was placed between the annular Si(Au) detector and the target to absorb the deuterons scattered from the target. As a consequence, the beam current could be increased, which rendered it possible to employ the swept-current mode of operation of the lens and to obtain good statistics for the entire coincidence spectrum. Of course, the energy resolution on the heavy-particle side was lost because of the absorber, but this was no serious limitation in the present case.

2.3. Lifetime-measurement methods with the cyclotron pulsed beam

2.3.1. Time structure of the ion beams from the Jyväskylä 90 cm cyclotron

As a consequence of the nature of the acceleration process in the cyclotron, the ion beam from this accelerator is bunched in short micropulses. The distance between these pulses (normally a time scale, i.e. the time of flight of the ions,is used) is related to the frequency of the accelerating rf voltage and to the harmonic mode of acceleration. Micropulses of the extracted ion beam can be shortened by phase

selection during the acceleration, i.e. (1) because of the phase shift, part of a micropulse gets into the decelerating part of the cycle; (2) the ion paths are radially limited in the beginning of the acceleration process. Because of the direction and the velocity distribution of the ions, micropulses are streched during the beam transport to the target. In lifetime measurements based on the use of a pulsed beam, the micropulses should be as short as possible.

The Jyväskylä 90 cm cyclotron MC-20 is a variable-energy sector-focused cyclotron for accelerating light particles to a maximum energy of 20 q^2/m MeV. It is a four-sector machine with two 90° dees, where protons and ^3He particles are accelerated usually in the first harmonic mode (push-pull), and deuterons and α particles in the second harmonic mode (push-push). In both acceleration modes are used rf frequencies of 10 to 26 MHz. In a normal run micropulses extracted from the cyclotron are very short, about 1-2 ns. This is caused by the central-region construction, which strongly defines the emittance, and by the phase selection during the acceleration and the extraction. In first-harmonic acceleration a set of phase slits can be employed to shorten the micropulses down to 0.5 ns. In practice, as in the present work, the same result was obtained with phase selection by detuning the cyclotron magnetic field.

The length of the beam transport line from extraction to the target chamber is about 25 m. The 90° analyzing magnet is a double-focusing magnet with a dispersion of 2.2 mm/‰ (energy) in the focal plane. The length of micropulses is mainly determined at the extraction, so that with a normal analyzing-slit combination of 1 × 1 mm, micropulses having a slope of 100 ps and a length of 500 ps can be obtained at the target.

In lifetime measurements based on the use of a pulsed beam, the time-to-pulse-height converter (TPHC) is stopped with a signal correlated with the beam pulse (the start signal being generated by the detector), which in this work is derived from a signal of the cyclotron rf. In addition to the normal nanosecond delay calibration, an rf calibration is used in the time calibration of TPHC, i.e. the time difference between the adjacent micropulses is detected. An accuracy of 1 % with these methods can easily be achieved.

2.3.2. A magnetic lens plus plastic scintillation detector spectrometer for in-beam lifetime measurements

The excellent time structure of the pulsed beam from the Jyväskylä cyclotron can be utilized best in lifetime measurements if the time delay distribution between the rf signals and the pulses from a fast plastic scintillation detector is measured. However, when γ rays are detected the use of a coincidence arrangement is necessary since the poorness of energy resolution of a plastic scintillator in γ-ray detection does not usually allow an identification of the transition. The energy resolution of about 20 % in conversion-electron detection is also insufficient.

In obtaining time information from conversion electrons, a plastic scintillation detector coupled to a magnetic spectrometer can be employed[15,16]. In this set-up the energy selection is performed by the magnetic spectrometer with a narrow momentum window. Of course,

the improvement of the momentum resolution takes place at the expense of the efficiency, which causes a relative increase of the background contribution. However, if the background is tolerable, the low efficiency in this kind of direct lifetime measurement with the pulsed beam is not a limitation since the beam current can be increased and the counting rate of the time spectrum is essentially the same as that of the singles spectrum of the spectrometer. This method is especially suited to the lifetime measurements of 0^+ states in which E0 conversion electrons are detected in the high-energy part of the electron spectrum with a relatively low background.

In Jyväskylä a lens spectrometer identical to that described by Kleinheinz et al.[17], with a plastic scintillation detector in in-beam lifetime measurements, has been employed. In this spectrometer combination illustrated in fig. 4, the momentum resolution is determined by an adjustable ring-focus baffle. Special attention has been paid to the reduction of the background radiation from the target and the slits in the beam line. By using a small NE111 plastic scintillator (in this work 1 cm in diameter by 0.5 cm thick) directly attached to a 56AVP photomultiplier, the detection of the background radiation has been minimized and a good time resolution has been achieved. Furthermore, when the scintillator is thick enough to stop the detected electrons, an energy window on the total absorption "peak" has been used to eliminate the background events due to the neutrons and γ rays in the low-energy part of the spectrum (fig. 5).

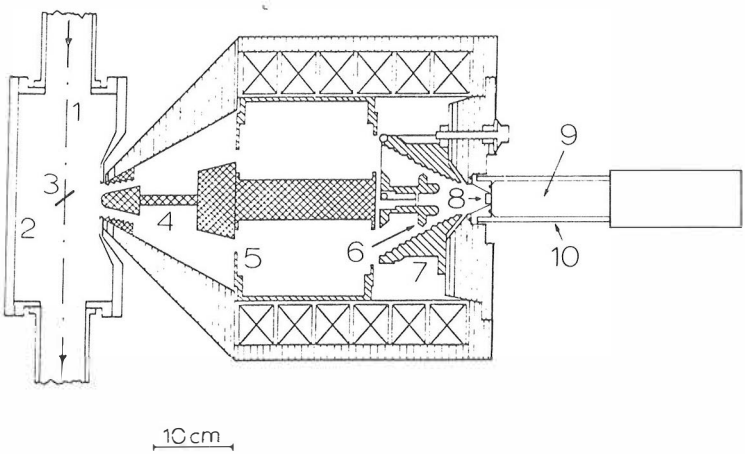

Fig. 4. Schematic cross-sectional diagram of the lens spectrometer plus plastic scintillation detector arrangement:
(1) beam, (2) target chamber, (3) target, (4) lead baffles, (5) aluminium baffles for positron-electron discrimination, (6) adjustable ring-focus baffle, (7) aluminium staircase, (8) plastic scintillator, (9) photomultiplier tube, (10) μ metal shield

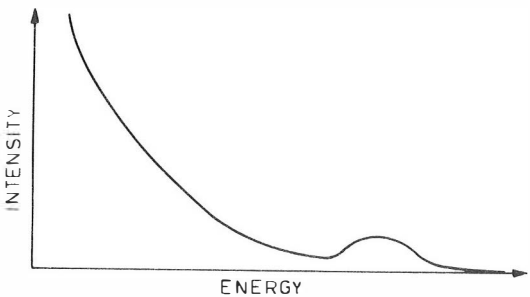

Fig. 5. Typical shape of spectrum obtained with the magnetic lens plus plastic scintillation detector

The time information has been derived directly from the anode pulse of the photomultiplier by means of the constant-fraction timing technique. The time resolution was mainly determined by the time structure of the beam pulses. When the slope method in the analysis of the time spectra is used, accurate determinations of half-lives longer than about 0.2 ns can be performed with this spectrometer arrangement. The uncertainty in determining the prompt contribution (mainly due to the continuum electrons) makes difficult the use of other methods in the analysis of the time spectra.

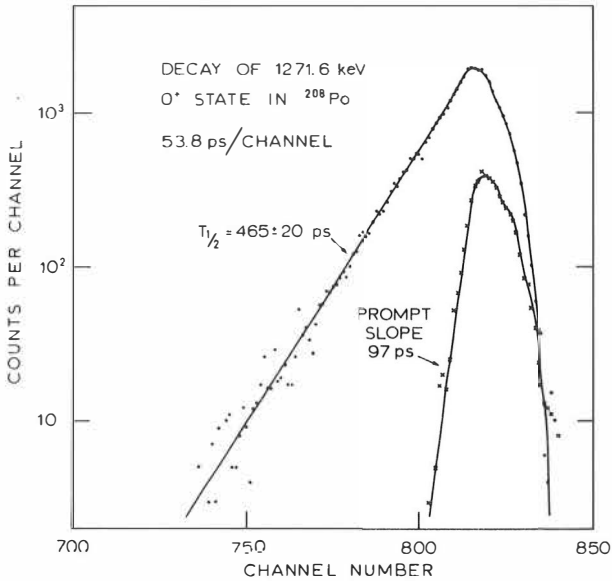

Fig. 6. Decay of the 1271.6 keV 0_2^+ state of ^{208}Po, populated in the reaction ^{209}Bi(p,2n). The constant background of 10 counts per channel has been subtracted.

In this work the spectrometer has been used in the measurements of the half-lives of the 0_2^+ levels in ^{206}Pb and ^{208}Po. Fig. 6 shows the result in the case of ^{208}Po, where the K conversion electrons associated with the E0 transition from the 1271.6 keV 0_2^+ state to the ground state were detected. The 0_2^+ level was populated in the reaction $^{209}Bi(p,2n)^{208}Po$ with 14.8 MeV protons. The thickness of the bismuth target was about 5 mg/cm^2 and it was evaporated on a 1 mg/cm^2 thick mylar backing. The momentum resolution of the lens was about 4 % (60 keV). The time structure of the beam was tuned by detuning the cyclotron magnetic field. The prompt shape was measured by detecting continuum electrons above the conversion electron lines associated with the 1272 keV E0 transition. The beam current was about 8 nA, and the time spectra shown in fig. 6 were obtained in four adjacent runs of 20 minutes.

2.3.3. The combination intermediate-image magnetic plus Si(Li) electron spectrometer in in-beam lifetime measurements

In lifetime measurements based on the detection of conversion electrons with a Si(Li) detector and on the use of a pulsed beam, a lower limit for the measurable half-lives is set by the timing properties of the Si(Li) detector. Depending on the energy of the transition, a prompt shape having a slope of about 0.5 ns and a FWHM of 2 to 4 ns can be obtained when ARC timing techniques are used. However, the advantage in the use of a cooled Si(Li) detector is the excellent energy resolution, which renders it possible to perform a two-parameter timing measurement

in which the time information from the TPHC and the corresponding energy information from the Si(Li) detector are stored event by event on a magnetic tape. This allows a subsequent analysis of the time spectra corresponding to different conversion electron lines and background events. Because the selection of a transition is carried out by the Si(Li) detector, a magnetic lens with a large momentum bandwidth in conjunction with the Si(Li) detector can be employed. The use of the swept-current mode in the lens is also possible.

In this work the combination intermediate-image magnetic plus Si(Li) electron spectrometer described in fig. 1 in subsect. 2.2.1 was employed in half-life measurements of 0_3^+ states in ^{112}Cd and ^{114}Cd.

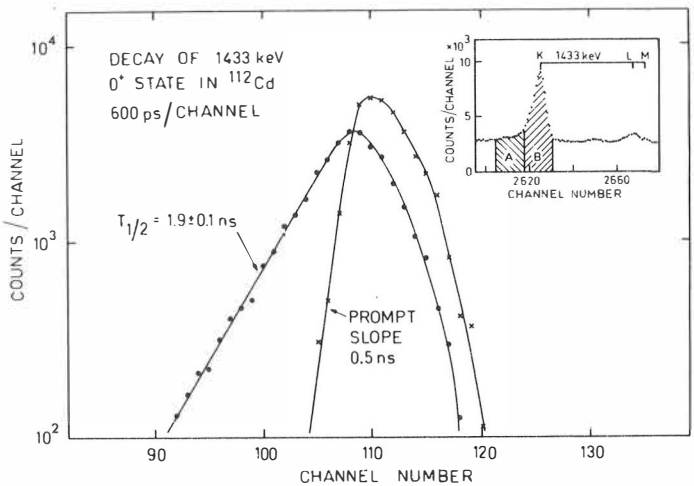

Fig. 7. Half-life measurement of the 1433 keV 0_3^+ state in ^{112}Cd. The time spectrum obtained by gating with the energy window A is subtracted from the time spectrum corresponding to window B.

Fig. 7 shows the result of a measurement in which the half-life of the 1433 keV 0_3^+ level in ^{112}Cd has been determined by analyzing the time spectrum corresponding to the K-line of the 1433 keV E0 transition in the conversion electron spectrum. In this experiment a ^{111}Cd target (0.8 mg/cm^2) was bombarded with 9 MeV deuterons and the 0^+ level was populated in the (d,p) reaction. The current of the magnetic lens was swept and the prompt shape was obtained with the aid of the prompt peak at 1373 keV. A half-life value, $T_{1/2}$ = 1.9±0.1 ns, for the 0_3^+ state in ^{112}Cd has been determined directly from the slope of the time spectrum.

Depending on the energy of the observed transition, half-lives down to about 1 ns can be determined directly from the slope with the present arrangement. By using the convolution method in the analysis, half-lives down to a few hundred picoseconds can be measured in favourable cases. Due to the statistical uncertainties in the determination of a centroid-walk curve[18], in practice the centroid-shift method does not improve the lower limit of the half-life to be determined.

In the direct lifetime measurements with a pulsed beam presented in this and the previous section, additional experimental or physical arguments are needed for the identification of the level responsible for the observed half-life. In the case of 0^+ levels a plausible argument could be the experimental observation that these levels usually are directly populated in the reaction and not in the decay of other states above them. The assignment of the half-life, determined in fig. 7, to the 1433 keV 0_3^+ level is also clear because of the absence of a prompt contribution in the time spectrum.

2.3.4. A walk-free centroid method for lifetime measurements with pulsed beams

The development of lifetime-measurement methods based on the use of the centroid shift method in the derivation of the lifetime from the time spectra is important because these methods usually cover a time region not achieved by other methods.

Both the Ge(Li) and the electron spectrometers are employed in conjunction with the centroid method[18-20]. In such experiments, half-lives well below 100 ps have been measured. However, problems arise from the centroid walk, i.e. the fact that the centroids of prompt transitions shift as a function of gamma-ray or electron energy. Furthermore, it is not always possible to definitely assign a measured half-life to the proper level.

A widely employed method is also the associated-particle timing technique[21], generally used in conjunction with DC beams. In this method, the level responsible for a half-life is identified with the aid of a peak in the associated charged-particle spectrum, taken in coincidence with the γ-ray spectrum. The most usual detector combination employed is a silicon semiconductor (for particles) and a scintillation detector (for γ rays). When the centroid-shift method is used, the walk problems are present, although less severe than in the cases mentioned above, and the time resolution of the system critically depends on the properties of the silicon detector.

In the present work, the associated-particle timing techniques have been developed further, on the basis of the use of very short

cyclotron micropulses.

In the present technique, the signal containing the time information is formed independently of the method of identifying the level associated with the half-life to be determined. This is accomplished by measuring the time delay between the rf signal from the cyclotron and a pulse from a plastic scintillation detector. That there is virtually no pulse-height-dependent walk in the centroid position is ensured by placing a fixed single-channel analyzer (SCA) window on the Compton distributions of the prompt and the delayed γ rays. In the most favourable cases, as in this work, the same γ ray is used in obtaining both the prompt and the delayed time distributions.

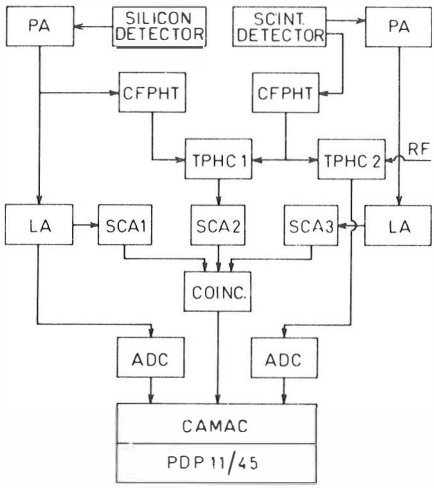

Fig. 8. Schematic block diagram of the walk-free centroid method

The nuclear energy levels are fixed by isolating the corresponding particle groups in the particle spectrum of a silicon detector operated in coincidence with the plastic scintillator.

A simplified schematic diagram of the present set-up is illustrated in fig. 8. The scintillation detector consists of a cylindrical (4.6 cm in diameter by 4.6 cm long) NE102A plastic scintillator coupled to a 56AVP photomultiplier, which is fast enough for the present purpose. This detector is placed at a distance of about 2 cm from the target, at 90° to the beam direction. The silicon detector is a 110 mm^2 x 3 mm Si(Li) counter, positioned at about 2.5 cm from the target, at an angle of 140°.

To a great extent fig. 8 is self-explanatory. However, some comments might be necessary: to minimize the number of random coincidences, the width of the coincidence window in SCA2 following TPHC1 must be smaller than twice the time interval between the micropulses (i.e. about 100 ns), and the prompt peak must be placed at the centre of the window. The particle signal from the Si(Li) detector and the time signal from TPHC2 are lead through the CAMAC interface to the computer. The data are collected event by event on a magnetic tape, for subsequent analysis.

A test of the walk-free centroid-shift method was performed by measuring the half-life of the 2032 keV ($\frac{1}{2}^{+}$) state of ^{209}Pb, for which a value of 161±8 ps is reported[22] from an off-line delayed-coincidence measurement employing the slope method. In the present experiment, an enriched, metallic self-supporting ^{208}Pb target (0.5 mg/cm^2) was bombarded with 10 MeV deuterons with a beam current of about 10 nA, and the states in ^{209}Pb were populated in the (d,p) reaction.

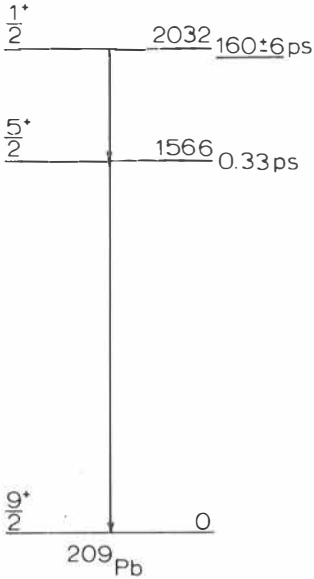

Fig. 9. Partial level scheme of ^{209}Pb and transitions relevant to the test measurement. The present half-life result (underlined) is included.

As the half-life of the $\frac{5}{2}^+$ state at 1566 keV (through which the 2032 keV state decays) is only 0.33 ps (ref. 23), the 1566 keV γ ray can be used to mark the decay of both states. In the measurement carried out, a 4 mm thick lead absorber was placed in front of the scintillator, to attenuate low-energy quanta. The width of the energy-selection window (SCA3 in fig. 8) on the Compton tail of the 1566 keV γ rays was about 50 %.

Fig. 10 a shows the coincidence axis of the particle spectrum obtained (the "all-coincidence" spectrum), and fig. 10 b the time distributions corresponding to the gates placed on the proton peaks associated with the population of the 2032 keV and 1566 keV levels.

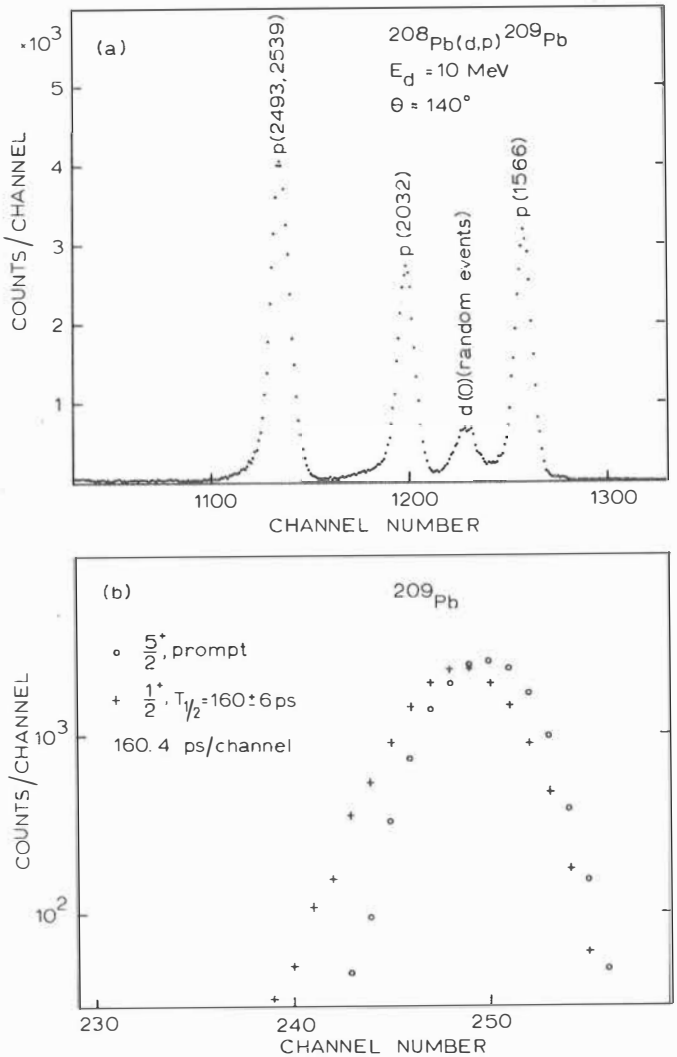

Fig. 10. a) Coincidence-axis particle spectrum from the reaction ^{208}Pb(d,p)^{209}Pb. The peaks are labelled by the ^{209}Pb energy levels populated. b) Delay-time distributions corresponding to the 1566 keV ($\frac{5}{2}^+$) and 2032 keV ($\frac{1}{2}^+$) levels in ^{209}Pb.

As can be inferred from the spectrum in fig. 10 a, the final time spectra contain only negligible fractions of spurious events. The corrections with respect to the random events were carried out using the area of the elastic (i.e. random) deuteron group d(0) of spectrum 10(a) and considering the fact that the shape of the random spectrum is the same as that of the gross spectrum. The contribution from the tails of the other peaks was estimated by investigating the effects associated with changing the width of the energy gate. The weighted average of half-life values given by the centroid-shift method and Newton's area-analysis method[24] for the 2032 keV state is 160±6 ps, which is in excellent agreement with the value of 161±8 ps in ref. 22. The same value is also obtained using a correct convolution method[25,26].

The walk-free centroid method is capable of obtaining half-life values in the 10 ps region. Another advantage of the method is that it inherently contains a way of identifying the level responsible for the observed half-lives. Furthermore, the time resolution is independent of the silicon detector and is mainly determined by the time structure of the beam. For that reason it is possible to use two independent silicon detectors to increase the coincidence efficiency, as was done in lifetime measurements of 0^+ levels in ^{116}Sn and ^{118}Sn.

Obviously, the method can be applied to reactions in which charged particles are emitted in such a way that the level density of the final nucleus is sufficiently low to allow a reasonable isolation of the different particle groups. Naturally, the level scheme must be well known, as well as the spectrum of the emitted particles. In practice, the particle detector is placed as close as possible to the target

in such a manner that the kinematic broadening of the peaks does not become too severe. An obvious limitation of the method is set by the maximum allowable counting rate of the particle detector, which in the present measurement was about 10^4 cps.

From the point of view of the analysis of the data, the events must be collected on a magnetic tape, so that different gate widths can be tried for a reliable elimination of the spurious events. To improve the flexibility and reliability of the method, the γ-ray energy information should also be recorded.

It should be pointed out that, in some cases, a spurious half-life result may arise from the following sequence of events: protons, first elastically scattered from the target, scatter inelastically in the silicon detector. The 2_1^+ state at 1.78 MeV in ^{28}Si is thereby excited and the de-excitation γ ray reaches the scintillation detector. Thus, an event is recorded which appears to correspond to a level at 1.8-1.9 MeV in the target nucleus. However, such false events are important only if the cross section of the reaction studied is extremely small. For example, in the measurements presented in this work, such spurious events can be ignored.

2.4. Double Coulomb excitation

Two-phonon-like levels in vibrational even-even nuclei, as Cd and Sn, are excited in double Coulomb excitation with heavy ions. Because of this fact, adapting this method to the determination

of absolute transition probabilities from 0_2^+ states in these nuclei is reasonable. However, in singles γ-ray spectra or in ordinary coincidence experiments, transitions from these weakly populated levels are usually difficult to observe and may be obscured by background lines.

In this work a high-efficiency coincidence method has been employed in double Coulomb excitation studies. This method was developed by N.-G. Jonsson, J. Kantele and A. Bäcklin and it is described in ref.27. In the experimental arrangement of this method, the target (usually thick) is placed very close to a 120 cm^3 Ge(Li) detector and both are surrounded by a large NaI(Tl) annular detector of the usual anti-Compton type. In studies of the even-even vibrational nuclei the $2_1^+ \rightarrow 0_1^+$ transition is detected by the NaI(Tl) annulus with an extremely high efficiency, and the coincidence transitions as well as the singles spectrum, for normalization purposes, are recorded by the Ge(Li) detector. The observation of the coincidence transitions renders it possible to determine the excitation cross sections of several weakly populated levels, such as the 0_2^+ levels, relative to the cross section of excitation of the 2_1^+ level, for which the reduced transition probability B(E2↑) usually is accurately known.

An accuracy of about 15 % in determining excitation cross sections with the present method can be achieved. The B(E2) values are obtained from the excitation cross sections by the use of the Winther de Boer computer code[28].

3. DECAY OF TWO-NEUTRON-HOLE 0_2^+ STATES IN ^{206}Pb AND ^{208}Po

3.1. Introduction

The nucleus $^{206}_{82}Pb_{124}$ has two neutron holes outside the doubly closed shells of ^{208}Pb, and it is widely believed that the lowest excited states of ^{206}Pb can be described in the simple shell-model picture as having a fairly pure two-neutron-hole character[29]. Such a state should also be the 1165 keV 0_2^+ state [30] in ^{206}Pb.

The nucleus $^{208}_{84}Po_{124}$ has two neutron holes and two proton particles outside the ^{208}Pb core. Since the same elementary mode of excitation as in ^{206}Pb is present at low energies in this nucleus, a 0^+ state much like that in ^{206}Pb should be found among the lowest excited states, where two-proton excitations can also be expected[32].

If the simple shell-model picture is valid, the E0 transition from the above-mentioned two-neutron-hole 0^+ states to the ground state is forbidden since the monopole matrix element, involving a sum over charged particles, vanishes. Consequently, the measurement of absolute values of these transition probabilities is of considerable interest since they are sensitive to changes of the proton core.

An unusually weak E2 transition from the 0_2^+ state to the 2_1^+ state in ^{206}Pb (E0/E2 $\geq$ 60) is reported in ref. 33. The half-life of this 0_2^+ state has also been measured previously with the aid of a Si(Li) detector plus a low-dispersion magnetic device in conjunction with a pulsed beam[34].

The situation in ^{208}Po has been rather unclear and the existing data[32,35] are not sufficient even for a firm identification of the 0_2^+ state. In ref. 35 a strong 1273±16 keV E0 transition and a 575±7 keV E2 transition from the 0_2^+ state in ^{208}Po are reported. The ratio of E0/E2 = 0.02, given in ref. 35, does not indicate a similarity of the 0_2^+ states in ^{206}Pb and ^{208}Po. In the investigation of states in ^{208}Po via the two-neutron pickup reaction ^{210}Po(p,t)^{208}Po, a level corresponding to the 0_2^+ state in ^{206}Pb is not seen[32]. On the other hand a line at 1263 keV is identified with a two-proton 2^+ state. The triton energy resolution in this experiment was about 12 keV.

3.2. Measurements and results

In this work a remeasurement of the half-life of the 0_2^+ level in ^{206}Pb has been carried out. The confusion associated with the identification and the decay of the 0_2^+ level in ^{208}Po has been cleared up and the half-life of this level has been measured.

In the half-life measurements, the magnetic lens plus plastic scintillation detector spectrometer described in subsect. 2.3.2 was employed with the pulsed beam of the cyclotron. In the case of ^{206}Pb the 1165 keV 0_2^+ state was excited in inelastic proton scattering. By choosing a bombarding energy of 12.30 MeV, which corresponds to a $1/2^+$ isobaric analog resonance[36] in ^{207}Bi, a factor of about five, as compared to other bombarding energies, is gained in the excitation cross section of the 0_2^+ state. A 10 mg/cm^2 thick enriched (90 %)

self-supporting metallic target was used. The K conversion electrons associated with the 1165 keV E0 transition were focused onto the small plastic scintillator, the momentum resolution of the lens being set at about 4 %. The result of this run is illustrated in fig. 11, where a constant background of 7 counts per channel has been subtracted from the delayed spectrum. The prompt component in the delayed spectrum corresponds to continuum electrons originated in the target, which was shown by setting the momentum window of the lens just below the E0 conversion electron lines and observing the corresponding time spectrum.

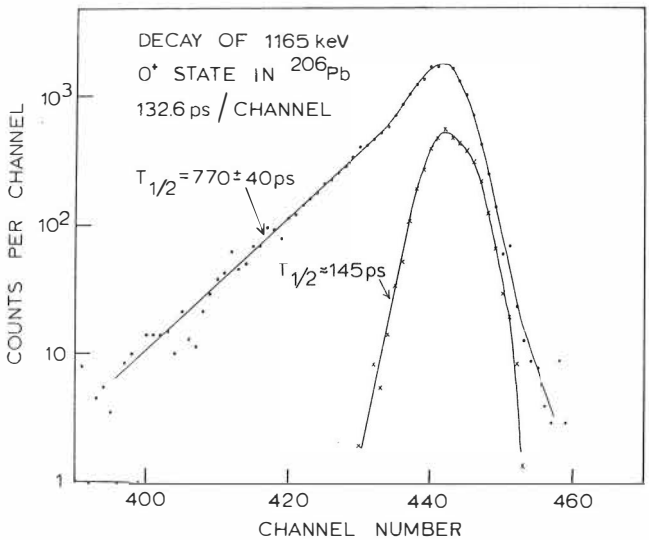

Fig. 11. Time-delay distributions between the K conversion electrons of the 1165 keV E0 and 803 keV E2 transitions in ^{206}Pb and the cyclotron beam pulse

The prompt shape in fig. 11 was obtained by detecting K conversion electrons from the prompt decay of the 803 keV 2_1^+ level. The present half-life value, $T_{1/2}$ = 770±40 ps, directly derived from the slope of the delayed spectrum, is in agreement with the value of 670±70 ps in ref. 34, where the more inaccurate convolution method was used.

The ρ^2 value derived from the present result is

$$\rho^2 = \ln 2/\Omega_K T_{1/2}(K) = (1.16\pm0.08)\cdot 10^{-3},$$

which gives a monopole strength value of ρ = 0.034±0.001. A partial half-life, $T_{1/2}(K)$ = 890 ps, is calculated by ignoring the E2 branch (E0/E2 > 60, ref. 33) and using the K/(L + M + ...) ratio for the E0 decay[37]. An electronic factor $\Omega_K = 6.7 \times 10^{11}$/s has been taken from ref. 37. From the upper limit for the intensity of the E2 transition, one obtains $B(E2;\ 0_2^+ \rightarrow 2_1^+) < 1.9 \times 10^{-52} e^2 cm^4$, or < 2.7×10^{-2} Weisskopf units.

In bombardments of an 800 $\mu g/cm^2$ bismuth target (evaporated on a thin mylar backing) with 14.8 MeV protons, a spectrum similar to that reported in ref. 35 was obtained by means of the ring-focus magnetic lens plus Si(Li) electron spectrometer mentioned in subsect. 2.2.1. An intense electron group corresponding to a transition energy of 1271.6±0.8 keV is assigned to an E0 transition because of the virtual absence of any possible corresponding γ-ray line. The half-life associated with the K conversion line of this transition, 465±20 ps, is obtained from the run described in subsect. 2.3.2 and illustrated in fig. 6.

Excitation-function runs clearly establish that the E0 transition takes place after the reaction $^{209}Bi(p,2n)^{208}Po$. A proper excitation

curve near the threshold could not be obtained because of the strong background from the (p,n) reaction. However, since the transition was clearly present in spectra taken at E_p = 11.65 MeV, two conclusions can be drawn: (i) The observed E0 transition depopulates a 0^+ level at 1271.6±0.8 keV; (ii) this level is primarily populated either directly from the (p,2n) reaction or from levels below 1.6 MeV. However, since no suitable levels appear to lie in the energy region in question[31], the former alternative is probably the right one. This is also supported by the shape of the delayed time spectrum in fig. 6, where only a weak prompt component caused by the continuum electrons is present. Consequently, the level, transition and half-life mentioned are sufficiently well established.

In γ-ray spectra, obtained with the 0.5 cm^3 LEPS-germanium detector and with a 40 cm^3 coaxial Ge(Li) detector, no transition corresponding to the energy difference 1271.6 - 686.6 = 585.0 keV (where 686.6 keV is the energy of the $2_1^+ \rightarrow 0_1^+$ transition) was observed, which is in contradiction to the result reported in ref. 35. From the γ-ray and electron spectra an intensity ratio of $E0(0_2^+ \rightarrow 0_1^+)/E2(0_2^+ \rightarrow 2_1^+) > 3.3$ was derived. Combining this result, the measured half-life, the K/(L + M +...) ratio for the E0 decay[37] and the electronic factor ($\Omega_K = 9.95 \times 10^{11}$/s, ref 37), a lower limit for the monopole strength, $\rho = 0.030$, is obtained. By ignoring the E2 branch of the decay of the 0_2^+ state an upper limit, $\rho = 0.037$, is obtained. From the measured half-life and the branching-ratio limit, the result $B(E2;\ 0_2^+ \rightarrow 2_1^+) < 4.0 \times 10^{-52} e^2 cm^4$ or $< 5.5 \times 10^{-2}$ W.u. is derived.

That different levels slightly below 1.3 MeV were observed in refs. 32 and 35 is obvious, since the γ-ray data[31] establish the

2_2^+ level at 1263.0 keV in agreement with ref. 32. This 2_2^+ state decays directly to the ground state and, on the basis of angular-correlation and conversion-coefficient measurements, via a principally M1 transition to the 2_1^+ state. It is obviously this M1 transition which is erroneously identified as the E2($0_2^+ \rightarrow 2_1^+$) transition in ref.35. On the other hand, the triton energy resolution in ref.32 is not sufficient to resolve a triton group corresponding to the weak population of the 1272 keV 0_2^+ state in the reaction ^{210}Po(p,t)^{208}Po, just close to the 2_2^+ peak.

3.3. Discussion

A summary of the present results is given in fig. 12. The results on the 0_2^+ states of ^{206}Pb and ^{208}Po are very much alike: the ρ values are virtually identical and the E2 transitions to the 2_1^+ state are strongly hindered. This indicates that in the $0_2^+ \rightarrow 0_1^+$ monopole transition, the two protons added to the ^{206}Pb core appear as mere spectators and evidently no strong two-proton admixture in the wave function of the 0_2^+ state in ^{208}Po is probable[31].

The hindrance of the E2 transition can be accounted for in the framework of shell-model wave functions and a neutron effective charge[34].

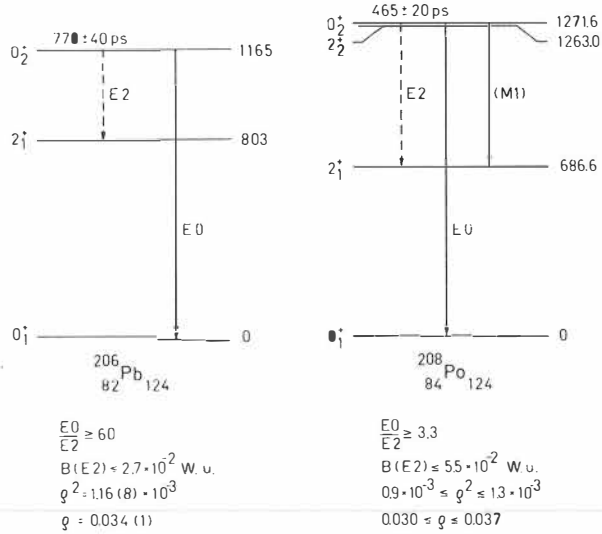

Fig. 12. Summary of the present results on the 0_2^+ states in ^{206}Pb and ^{208}Po

For pure two-neutron-hole 0^+ states the wave functions can be written as follows:

$$0_1^+ = \sum_j A_j \, (j^{-2})^0 \, , \quad 0_2^+ = \sum_j B_j \, (j^{-2})^0 \, ,$$

where j represents neutron single-particle states and $\sum_j A_j B_j = 0$ by orthogonality. For this reason, if we are limited to a single major shell, the E0 transition matrix element

$$\langle 0_1^+ \mid \sum_i e_i r_i^2 \mid 0_2^+ \rangle = -2 \sum_j A_j B_j \langle j \mid e_j r_j^2 \mid j \rangle$$

is nonzero only if the neutron effective charge e_j is j-dependent (for the harmonic oscillator model $\langle j \mid r^2 \mid j \rangle$ is independent of j within a major shell). A state-dependent monopole effective charge has been introduced by Tape et al. in ref.34.

The monopole matrix element for a neutron in the state j is

$$\langle j \mid e_j r_j^2 \mid j \rangle = Z \, \delta \langle r^2 \rangle ,$$

where $\delta \langle r^2 \rangle$ is the change of the mean-square charge radius of the nucleus when a neutron is added to the system (valence neutrons in the state j in both systems) and it can be derived from the isotope shift between adjacent isotopes of an element. Consequently, the E0 transition matrix element can be calculated if the components of the wave functions of the 0^+ states and the isotope shifts associated with the single-particle matrix elements are known.

In ref.34 wave functions including only $p_{1/2}$ and $f_{5/2}$ components are used in the calculation of the E0 transition probability in ^{206}Pb. The matrix element for the $p_{1/2}$ neutron has been obtained from the $\delta \langle r^2 \rangle$ value corresponding to the ^{207}Pb-^{208}Pb isotope shift (a neutron added to the $p_{1/2}$ orbit). The matrix element for the $f_{5/2}$ neutron has been obtained by taking one-half of the $\delta \langle r^2 \rangle$ value corresponding to the ^{204}Pb-^{206}Pb isotope shift. The E0 transition matrix element includes the difference of the $f_{5/2}$ and $p_{1/2}$ matrix elements, i.e. the difference of the corresponding $Z \, \delta \langle r^2 \rangle$ values. Since the $Z \, \delta \langle r^2 \rangle$ values are of the same order of magnitude, it is evident that even small inaccuracies in the isotope shifts produce a large uncertainty

in the E0 transition matrix element. Furthermore, on the basis of the isotope-shift data it can be noted that the use of half of the δr^2 value corresponding to the ^{204}Pb-^{206}Pb isotope shift instead of the δr^2 value corresponding to the unknown ^{205}Pb-^{206}Pb isotope shift makes the whole calculation meaningless. The same difficulties are encountered if the most accurate data obtained in muonic-atom measurements[39] are used.

As we lack the experimental isotope shifts it is more reasonable to use theoretical calculations. J. Speth et al.[40] have calculated isotope shifts of neutron-hole states in ^{207}Pb relative to ^{208}Pb by applying the theory of finite Fermi systems. Using these values and shell-model wave functions for the 0^+ states of ^{206}Pb calculated by True[29] ($A_{1/2}$ = 0.822, $A_{5/2}$ = 0.401, $A_{3/2}$ = 0.363, $A_{13/2}$ = -0.109, $A_{7/2}$ = 0.130, $A_{9/2}$ = 0.059; $B_{1/2}$ = 0.495, $B_{5/2}$ = -0.834, $B_{3/2}$ = -0.090, $B_{13/2}$ = 0.152, $B_{7/2}$ = -0.145, $B_{9/2}$ = -0.083), a value of 0.50 fm^2 for the E0 transition matrix element, i.e. 0.010 for the monopole strength ρ, is obtained. If only the $p_{1/2}$ and $f_{5/2}$ components of the wave functions are used, the resulting ρ value is 0.023. Using wave functions calculated by Ma and True[41] ($p_{1/2}$, $f_{5/2}$ and $p_{3/2}$ components for the 0_2^+ state in ^{206}Pb are reported) a ρ value of 0.027 is obtained. Although this value would be smaller if other components of the wave functions could be taken into account, it is rather close to the present experimental value of ρ = 0.034±0.001.

Isotope shifts between the Po isotopes are unknown, but identical ρ values for the present E0 transitions indicate that isotope shifts associated with the E0 transition in ^{208}Po should be very similar to those of the Pb isotopes.

4. DECAY OF 0_2^+ AND 0_3^+ STATES IN EVEN Sn NUCLEI

4.1. Introduction

In most theoretical studies of the levels of even Sn nuclei, neutron excitations in the framework of the quasiparticle models are considered[3,42-46]. A reasonable agreement with the experimental energy spectra and two-neutron transfer cross sections is achieved in two-quasiparticle calculations assuming an inert Z = 50 core. However, in a more adequate description of the more collective 2_1^+ and 3^- states, excitations of the core are needed[42]. On the other hand, the existence of the low-lying 0^+ states found in several Sn isotopes has been difficult to explain within the neutron-quasiparticle models.

A new idea on the character of the low-energy 0^+ states in Sn nuclei has been produced by the observation of the strong population of the lowest excited 0^+ states of several Sn isotopes in the (^{3}He,n) reaction[47] and by the recent discovery of quasi-rotational bands[48] evidently based on the 0_2^+ states. The (^{3}He,n) results and the similarity of the observed bands with the ground-state bands of the Pd and Xe isotones clearly indicate that the low-lying 0^+ states (at least the 0_2^+ state) in Sn nuclei originate at least partially from a nonclosed Z = 50 shell.

The excited states of even Sn nuclei have been intensively studied experimentally, e.g. in various one- or two-nucleon transfer

reactions[49,50], from the decay of Sb and In nuclei, and by means of in-beam γ-ray spectroscopy with the (α,2n) reaction[51]. However, except for the 2_1^+ and 3^- states, no information exists on absolute electromagnetic transition probabilities. The main body of information on the 0^+ states has been obtained from two-particle transfer reactions[50,52]. Information on the E0 and E2 decay properties of the 0^+ states would be of great value for the description of these states.

Previously, an E0/E2 ratio from the 0_2^+ state in ^{116}Sn (refs. 53, and 54) and preliminary results on the E0 and E2 branching ratios in ^{118}Sn (ref. 55) have been reported.

In this work a systematic study of the decay properties of the 0_2^+ and 0_3^+ states in even Sn isotopes has been carried out with the help of the methods described in sect. 2.

The even Sn isotopes are a good subject for a systematic investigation of the E0 transitions. In ^{114,116,118,120}Sn one can find two well-identified low-lying 0^+ states, which can de-excite only via an E2 transition to the 2_1^+ state or via an E0 transition to the ground state; furthermore, also an E0 transition proceeds between these excited 0^+ states. The 0^+ states in the Sn nuclei are populated in various reactions and in some cases also in the decay of Sb and In nuclei. Since metallic Sn targets from ^{112}Sn up to ^{124}Sn are available, inelastic proton scattering, usually at proton energies which correspond to $\ell_p = 0$ isobaric analog resonances (IAR)[56], was mostly used in this work.

4.2. Measurements

Experimental results of this work on even Sn nuclei are presented in fig. 15 and also in table 1 of section 4.3.

Singles spectra: In most experiments self-supporting enriched metallic ^{112}Sn (80.5 %), ^{114}Sn (64.1 %), ^{116}Sn (95.6 %), ^{118}Sn (97.1 %) and ^{120}Sn (98.4 %) targets were used. In the measurements of singles γ-ray and conversion-electron spectra, these targets were bombarded with proton beams of 7, 6.40 (IAR), 6.93 (IAR), 7.3 and 10 MeV proton energies, respectively, from the Uppsala EN Tandem. The 0^+ states were excited in the (p,p') reaction except in ^{118}Sn and ^{120}Sn, where the β^+ decays of the 3.6 min ^{118}Sb and 15.9 min ^{120}Sb produced in the (p,n) reaction were used.

In obtaining the singles conversion-electron spectra the ring-focus lens plus Si(Li) electron spectrometer (subsect. 2.2.1) in the swept- and fixed-current modes of operation was employed. Typical electron spectra are illustrated in refs. 57, 58. From these spectra, $E0(0_2^+ \rightarrow 0_1^+)$ transitions in all the isotopes and $E0(0_3^+ \rightarrow 0_1^+)$ transitions in ^{116}Sn, ^{118}Sn and ^{120}Sn are identified. The intensities of the competing E2 transitions are also taken from these spectra except in the ^{112}Sn case, where the complexity in this part of the spectrum disturbs the analysis, and in the ^{120}Sn case, where these transitions cannot be identified due to the β^- spectrum following the decay of an isomeric state in ^{120}Sn. In these cases the singles γ-ray spectra were used.

e^-p coincidence measurements: With the aid of the electron - heavy-particle coincidence arrangement it was possible to identify low-energy

E0 transitions between the 0_3^+ and 0_2^+ states in all the isotopes except ^{112}Sn. These experiments were similar to that in the ^{116}Sn case, which is described in subsect. 2.2.2. In the ^{114}Sn case the same target and the same energy of the proton beam from the cyclotron were used as in the measurements of singles spectra. The 0_3^+ state in ^{118}Sn was populated in the (d,p) reaction. An enriched (86 %) ^{117}Sn target of 0.8 mg/cm^2 thickness on a thin carbon backing and a 7 MeV deuteron beam from the cyclotron were used. In the case of ^{120}Sn a 0.5 mg/cm^2 thick target and inelastic proton scattering at an ℓ_p = 0 IAR energy of 7.64 MeV were used. For determining the branching of the E0($0_3^+ \rightarrow 0_2^+$) transitions, also the conversion electrons of the E2($0_3^+ \rightarrow 2_1^+$) transitions were observed in these coincidence runs except in the case of ^{114}Sn, where the E2($0_2^+ \rightarrow 2_1^+$) transition was detected.

Coulomb excitation: In double Coulomb excitation measurements thick (~15 mg/cm^2) enriched metallic Sn targets were bombarded with a 48 MeV ^{16}O beam from the Uppsala Tandem and the high-efficiency coincidence method (sect. 2.4) was employed. In these measurements E2 transition de-exciting the 0_2^+ states were identified in all the isotopes except ^{112}Sn and, consequently, B(E2) values and half-lives of these 0_2^+ states were determined. Upper limits of B(E2) values, i.e. lower limits of half-lives, were obtained for the other 0^+ states.

Direct half-life measurements on ^{116}Sn and ^{118}Sn: In determining the half-lives of the 0_2^+ and 0_3^+ levels in ^{116}Sn the walk-free centroid method described in subsect. 2.3.4 was successfully applied.

The equipment and geometry in this measurement were similar to those described in subsect. 2.3.4 except that two independent Si(Li)

particle detectors were used to increase the coincidence efficiency. The 0^+ states were excited in the (p,p') reaction with the 6.93 MeV IAR energy of the protons. The time structure of the pulsed beam was tuned by detuning the cyclotron magnetic field. The target was an enriched ^{116}Sn metallic foil of about 1 mg/cm^2 thickness. The depopulating γ ray of the "prompt" 2_1^+ state at 1293.5 keV ($T_{1/2}$ = 0.362 ps) was used to mark the decay of the 0_2^+, 0_3^+ and 2_1^+ states. To prevent the depopulating γ rays of the 0^+ states from being accepted by the scintillation detector, the threshold of the energy window (50 % in SCA3 of fig. 8) was placed well above their Compton edges. A 4 mm thick lead absorber was also placed in front of the scintillator to absorb low-energy γ rays.

The excitation cross-section of the 0^+ states is so small (100 μb/st at backward angles[59]) that the relevant proton groups cannot be resolved in the total particle spectrum of one of the Si(Li) detectors illustrated in fig. 13 a; the coincidence-axis spectrum of fig. 13 b demonstrates the selectivity of the coincidence method. Of course, a singles proton spectrum with a good resolution, i.e. with a longer distance between the Si(Li) detector and the target, was observed to make sure that no weak proton group unresolved in the spectrum of fig. 13 b disturbs the half-life determination.

In fig. 14 a and b the time spectra of the 0_2^+ and 0_3^+ states are shown together with the prompt resolution function corresponding to the 2_1^+ state. The greatest uncertainties in this measurement are associated with the subtraction of the random components in the time spectra (cf. the correction methods described in subsect. 2.3.4). The results obtained are: $T_{1/2}$ = 45±10 ps for the 0_2^+ state and $T_{1/2}$ = 160±20ps for the 0_3^+ state.

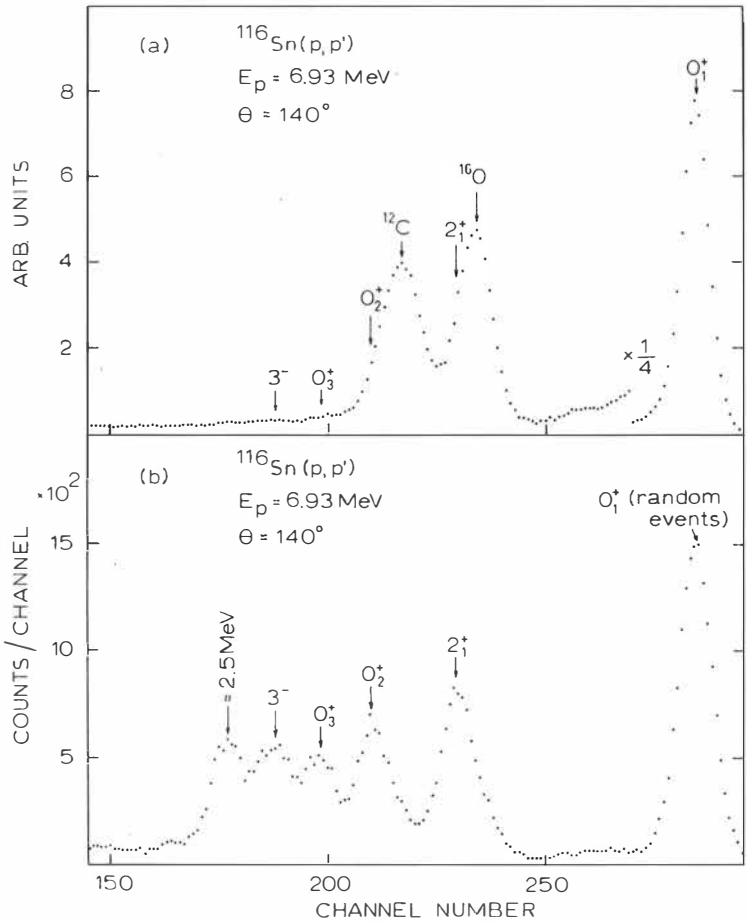

Fig. 13. Proton spectra of one of the Si(Li) detectors in the lifetime measurement with the walk-free centroid method.
a) Total particle spectrum. b) The corresponding coincidence-axis spectrum. The measurement time 18 h.

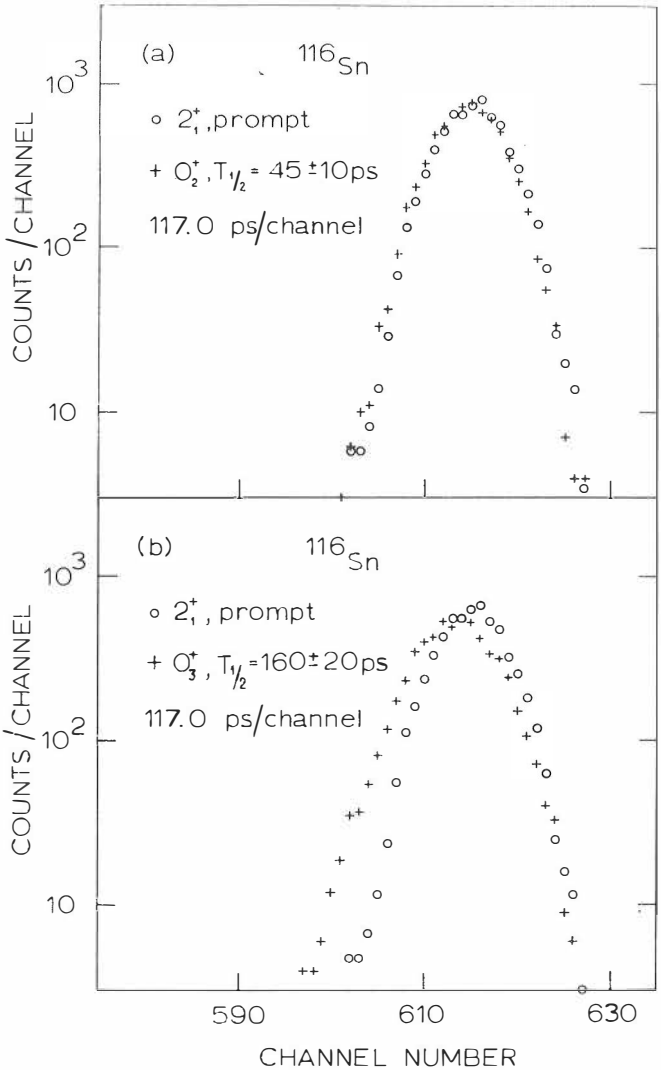

Fig. 14. Time delay distributions corresponding to the decay of the 0_2^+, 0_3^+ and 2_1^+ states in ^{116}Sn measured with the walk-free centroid method

The walk-free centroid method was also applied to obtain an upper limit for the half-life of the 0_3^+ state in ^{118}Sn: $T_{1/2}$ (0_3^+) < 200 ps. The ^{117}Sn(d,p)^{118}Sn reaction with a 10 MeV deuteron energy was used in this experiment. In spite of the use of a larger scintillation detector (NE102A: 10 cm in diameter by 10 cm long + XP2040) and two particle detectors, the statistics gathered in this experiment are not sufficient for determining an exact half-life value.

In the following some details of the present results on different isotopes are described.

^{112}Sn: No low-lying 0^+ levels previous to the measurements of the present work have been reported in this nucleus. The final level energy of 2190.9 keV is derived from the coincidence γ-ray spectrum taken with the γp coincidence set-up described in subsect. 2.1. This energy is in agreement with the recent result of 2.19 MeV derived from the (^{3}He,n) study (neutron energy resolution about 400 keV)[47]. No candidates for other low-lying 0^+ levels (≤ 3 MeV) were observed in the present measurements.

^{114}Sn: From the singles electron spectrum a ratio of $I_K(E0;\ 0_2^+ \to 0_1^+)/I_K(E2;\ 0_2^+ \to 2_1^+) = 1.00 \pm 0.20$ was obtained. The $E0(0_3^+ \to 0_1^+)$ transition from the known 2155 keV 0^+ level[50] was not observed: $I_K(E0;\ 0_3^+ \to 0_1^+)/I_K(E0;\ 0_2^+ \to 0_1^+) < 0.05$. Both the 0_2^+ and 0_3^+ levels were seen in the γp' coincidence spectrum, the depopulating γ rays having energies (intensities) of 856.2±0.8 keV (100) and 653.0±0.5 keV (135). From the e^-p coincidence measurement a ratio

of $I_K(E0;\ 0_3^+ \rightarrow 0_2^+)/\ I_K(E2;\ 0_2^+ \rightarrow 2_1^+) = 0.6\pm0.2$ was obtained. All these experiments were carried out with the same bombarding proton energy. Combining these results, the values in table 1 can be derived.

The same result for the E0/E2 branching ratio from the 0_2^+ state was also obtained in a measurement where singles electron and γ-ray spectra from the $^{115}In(p,2n)^{114}Sn$ reaction were observed. A 15 MeV proton beam from the cyclotron was used in this experiment.

Several attempts were made to observe a 0^+ state at 1.58 MeV, reported by Schneid et al.[49] and discussed by Rasmussen[3]. No trace of such a level was observed; Coulomb excitation results set a lower limit of about 6 ns for the half-life of a state near 1.58 MeV.

^{116}Sn: The (p,p') reaction through the $\ell_p = 0$ IAR was especially useful in this case. A factor of about four was gained in the population of the 0^+ states as compared to other proton energies.

After the identification of the $E0(0_3^+ \rightarrow 0_2^+)$ transition from the e^-p coincidence spectrum, the ratio $I_K(E0;\ 0_3^+ \rightarrow 0_2^+)/I_K(E0;\ 0_3^+ \rightarrow 0_1^+)$ can be taken in this case also from the singles electron spectrum. The resulting value of 15±1 (table 1) is in good agreement with the value 16±6 obtained from e^-p coincidence spectra.

The present E0/E2 ratio from the 0_2^+ state is in good agreement with that of ref.53 and is about 20 % higher than that of ref. 54 .

Several absolute E2 transition rates in ^{116}Sn were determined in double Coulomb excitation experiments. These results are presented and discussed in ref.60. The half-life of the 0_2^+ state, $T_{1/2} = 42\pm8$ ps, derived from these measurements agrees well with the former result

from the direct half-life measurement. However, before deriving this value a coherent interference between the main term and the term of the type $M_{0_1 2_1} M_{2_1 0_2} M_{0_1 2_2} M_{0_2 2_2}$ must be assumed in the calculation of the B(E2) value. In obtaining this term the known branching ratio[61] and the measured excitation cross section of the 2_2^+ level are used ($B(E2;\ 2_2^+ \rightarrow 0_2^+) = 0.058\ e^2b^2$).

<u>^{118}Sn:</u> The present branching ratios are in agreement with those of ref. 55.

<u>^{120}Sn:</u> In the singles conversion-electron spectrum the E2 transitions from the 0^+ levels were obscured by the β^- spectrum ($Q_{\beta^-} \approx 1$ MeV) following the decay of an isomeric state in ^{120}Sb, which has not been observed previously.

4.3. Results

In fig. 15 are presented the energy systematics, half-lives and transition intensities determined in this work for low-lying 0^+ levels in even-mass $^{112-120}$Sn.

The energies of the 0_2^+ and 0_3^+ levels, the ratios of the K conversion-electron intensities and the ratios of the reduced transition probabilities are collected in table 1. In table 2 the absolute transition rates and half-lives are presented.

$X\left(\frac{E0;0_3^+-0_2^+}{E2;0_3^+-2_1^+}\right)$		0.9	6.8	3.4	8
$X\left(\frac{E0;0_3^+-0_1^+}{E2;0_3^+-2_1^+}\right)$		<0.01	0.066	0.10	0.22
$X\left(\frac{E0;0_2^+-0_1}{E2;0_2^+-2_1^+}\right)$	0.046	0.042	0.0086	0.0096	0.0070

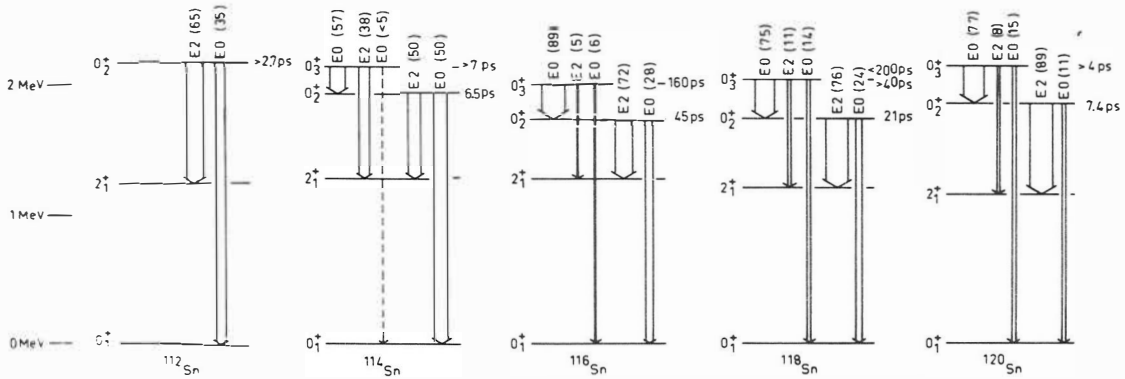

Fig. 15. Summary of the present results. Branching ratios of K conversion-electron intensities are shown in per cent in parenthesis.

Table 1. Summary of level energies and branching ratios [d)]

	0_2^+			0_3^+						
	Energy (keV)	$\frac{I_K(0_2^+\to 0_1^+)}{I_K(0_2^+\to 2_1^+)}$	$X\left(\frac{E0;0_2^+\to 0_1^+}{E2;0_2^+\to 2_1^+}\right)$	Energy (keV)	$\frac{I_K(0_3^+\to 0_1^+)}{I_K(0_3^+\to 2_1^+)}$	$X\left(\frac{E0;0_3^+\to 0_1^+}{E2;0_3^+\to 2_1^+}\right)$	$\frac{I_K(0_3^+\to 0_2^+)}{I_K(0_3^+\to 2_1^+)}$	$X\left(\frac{E0;0_3^+\to 0_2^+}{E2;0_3^+\to 2_1^+}\right)$	$\frac{I_K(0_3^+\to 0_2^+)}{I_K(0_3^+\to 0_1^+)}$	$\frac{\rho^2(0_3^+\to 0_2^+)}{\rho^2(0_3^+\to 0_1^+)}$
^{112}Sn	2190.9[a)]	0.55(10)	0.046(8)[c)]							
^{114}Sn	1953.0[a)]	1.00(20)	0.042(8)[c)]	2156.2[a)]	< 0.14	< 0.01	1.5(5)	0.9(3)	> 12	> 100
^{116}Sn	1756.8[b)]	0.38(8)	0.0086(18)	2027.3[b)]	1.18(20)	0.066(11)	18(3)	6.8(11)	15(1)	108(8)
^{118}Sn	1757.8[b)]	0.32(6)	0.0096(18)	2056.5[b)]	1.3(5)	0.10(4)	7(3)	3.4(15)	5(3)	34(20)
^{120}Sn	1874.0[a)]	0.12(3)	0.0070(18)	2158.9[a)]	2.0(4)	0.22(5)	10(4)	8(3)	5(2)	40(20)

a) From the present work. Typical error 0.5 keV.

b) From Nuclear Data Sheets, (refs. 62,63.)

c) Lowest observed excited 0^+ state in this work.

d) Uncertainty of the last figures in parentheses.

The experimental ratio of the reduced E0 and E2 transition probabilities X is obtained from the relation[64)]

$$X(0_i^+ \to 0_f^+) = X\left(\frac{E0;0_i^+ \to 0_f^+}{E2;0_i^+ \to 2_1^+}\right) = 2.56\cdot 10^9\ A^{4/3}\cdot \frac{I_K(0_i^+ \to 0_f^+)}{I_K(0_i^+ \to 2_1^+)}\cdot \frac{\alpha_K}{\Omega_K}\cdot E_\gamma^{\ 5},$$

where α_K is the theoretical K conversion coefficient[65)], Ω_K the electronic factor for the E0 transition[37)] and E_γ the energy of the E2 transition in MeV.

The experimental results can be summarized as follows:

<u>The ratios of the reduced transition probabilities</u> $X(0_2^+ \to 0_1^+)$ for $^{116,118,120}Sn$ are quite close to the theoretical value for a spherical vibrator[66)] for which $X = \beta_{rms}^2 \simeq 0.013$, where β_{rms} is taken from ref. 67. A change to about a factor of five larger values is observed in ^{114}Sn and ^{112}Sn.

The $X(0_3^+ \to 0_1^+)$ value decreases from 0.22 to 0.07 in going from ^{120}Sn to ^{116}Sn and is 8 to 30 times larger than the $X(0_2^+ \to 0_1^+)$ value in these isotopes. In ^{114}Sn $X(0_3^+ \to 0_1^+)$ falls down to a value of < 0.01, which is considerably smaller than $X(0_2^+ \to 0_1^+)$ in this nucleus. Such a behaviour would indicate an inversion of the 0_2^+ and 0_3^+ states in going from the heavier Sn isotopes to ^{114}Sn. However, the systematics of the B(E2) and ρ^2 values do not support this conclusion.

A very strong E0 transition between the excited 0^+ states is revealed by the large $X(0_3^+ \to 0_2^+)$ value, which does not show any systematic trend in $^{116,118,120}Sn$ but is noticeably smaller in ^{114}Sn than in the heavier isotopes.

The strength of the $E0(0_3^+ \to 0_2^+)$ transition as compared with the competing E0 transition to the ground state can be deduced from the $\rho^2(0_3^+ \to 0_2^+)/\rho^2(0_3^+ \to 0_1^+)$ value. An increase of this ratio towards lighter isotopes is evident.

The absolute transition rates in table 2 reveal the collectivity of the 0_2^+ states: the value of $B(E2;\ 0_2^+ \to 2_1^+)$ is of the order of 20 W.u. in $^{114,116,118}Sn$ ($\sim 1.5 \times B(E2;\ 2_1^+ \to 0_1^+)$). The ρ^2 value in $^{116,118,120}Sn$ is about one-half of the spherical vibrator value of about† 10×10^{-3} ($\rho_{vibr} = 0.151\ Z\beta^2_{rms}$, ref. 66). In going to ^{114}Sn, $E0(0_2^+ \to 0_1^+)$ suddenly gets stronger , which also was indicated by the increase of the X value.

The E2 transition from the 0_3^+ states is of the order of 1 W.u. and also the E0 transition to the ground state is weaker than that from the 0_2^+ states, being of the same magnitude as that from the two-neutron-hole 0^+ states in ^{206}Pb and ^{208}Po. The $0_3^+ \to 0_2^+$ transition is exceptionally strong, ρ^2 in ^{116}Sn being 10 times the spherical vibrator value and of the same order as the ρ^2 of the E0 transition from the β band head in deformed nuclei[1,68].

Concerning the systematic trends of the E0 and E2 transition rates, the following conclusions from the present results can be drawn:

(i) The $E0(0_2^+ \to 0_1^+)$ transition becomes markedly stronger in going to ^{114}Sn.

(ii) The $E2(0_3^+ \to 2_1^+)$ and $E0(0_3^+ \to 0_2^+)$ transitions become stronger and/or the $E0(0_3^+ \to 0_1^+)$ transition becomes weaker with decreasing mass number. Furthermore, in going from ^{116}Sn to ^{114}Sn this change is exceptionally strong and takes place in such a way that the strength of the $E2(0_3^+ \to 2_1^+)$ transition with respect to the $E0(0_3^+ \to 0_2^+)$ transition increases.

These trends can be roughly seen even in fig. 15.

---

† 10^{-3} is used as a suitable "unit" for ρ^2.

Table 2. Electromagnetic decay of 0^+ states in even Sn nuclei

A	112	114	116	118	120
$\frac{B(E2;\ 0_2^+\to 2_1^+)}{B(E2)_{W.u.}}$ a)	< 9	22(9)	17(4) b)	18(3)	13(2)
$T_{1/2}(0_2^+)$(ps) a)	> 2.7	6.5(23)	45(10) b)	21(3)	7.4(10)
$\frac{B(E2;\ 0_3^+\to 2_1^+)}{B(E2)_{W.u.}}$ a)	-	< 5	0.49(6) b)	<1.0 >0.2 b)	< 4
$T_{1/2}(0_3^+)$(ps) a)	-	> 7	160(20) b)	< 200 b) > 40	> 4
$\rho^2(0_2^+\to 0_1^+)\cdot 10^3$	< 12	26(13)	4.3(13)	5.2(13)	2.6(7)
$\rho^2(0_3^+\to 0_1^+)\cdot 10^3$	-	< 1.5	0.93(20)	< 4.1 > 0.4	< 30
$\rho^2(0_3^+\to 0_2^+)\cdot 10^3$	-	< 130	100(22)	< 140 > 11	< 1300
$\rho(0_2^+\to 0_1^+)$	< 0.15	0.16(4)	0.066(11)	0.072(10)	0.051(7)
$\rho(0_3^+\to 0_1^+)$	-	< 0.04	0.030(3)	< 0.064 > 0.02	< 0.18
$\rho(0_3^+\to 0_2^+)$	-	< 0.36	0.32(4)	< 0.38 > 0.10	< 1.1

a) Values derived from the Coulomb excitation measurements, except those labelled by b). Calculations made under the assumption that the interference due to the term of the type $M_{0_1 2_1} M_{2_1 0_2} M_{0_1 2_2} M_{0_2 2_2}$ is constructive and that $B(E2;\ 2_2^+ \to 0_2^+) = 0.058\ e^2 b^2$ (the same as for ^{116}Sn). Changing the sign of this term implies that the values of $B(E2;\ 0_2^+ \to 2_1^+)$ will increase ($T_{1/2}$ will decrease) as follows: ^{112}Sn, 23 %; ^{114}Sn, 27 %; ^{116}Sn, 40 %; ^{118}Sn, 33 %; ^{120}Sn, 70 %. If $B(E2;\ 2_2^+ \to 0_2^+) = 0$ the increase will be approximately half of the figures given. This uncertainty has not been included in

the errors given. For the B(E2; $0_3^+ \rightarrow 2_1^+$) values destructive interference has been chosen in order to give maximum values of the upper limits.

b) Values from direct half-life measurements.

c) $B(E2)_{W.u.} = 5.94 \cdot 10^{-6} A^{4/3} e^2 b^2$.

4.4. Discussion

The X, B(E2) and ρ^2 values associated with the 0_2^+ states in even Sn nuclei are roughly in accordance with those for a two-phonon 0^+ state of the spherical vibrator. The decay properties of the 0_3^+ states could be associated with a three-phonon 0^+state, except the strong $0_3^+ \rightarrow 0_2^+$ transition,which should be forbidden in this model. The low energy of the 0_3^+ states could be explained as being due to γ softness[9]. An inversion of two- and three-phonon 0^+states, suggested to take place throughout the tin region in ref.69, is not supported by the present results.

Since two-quasiparticle and other modes of excitation are present near 2 MeV in even Sn nuclei, more complicated explanations must be sought. The collectivity of the 0_2^+ states cannot be reproduced in the neutron quasiparticle calculations[43]. Proton excitations and a possible deformation in even mass Sn nuclei are indicated by the recently discovered quasirotational bands[48] (the proposed band members down to the 0_2^+ state are populated only in the case of ^{116}Sn).

The picture of low-lying proton excitations is also supported by the (^{3}He,n) study[47]. Furthermore, recent calculations[70,71] indicate that a proton pair promoted to the next major shell yields a low-lying 0^+ state with a deformation of about $\beta = 0.1$ in even Sn nuclei.

In the present double Coulomb excitation study of ^{116}Sn, a value of $B(E2;\ 2_2^+ \rightarrow 0_2^+) = 17$ W.u. was obtained for the E2 transition between the two lowest members of the proposed band[60]. The deformation parameter β_2 as deduced from this value is $\beta_2 = 0.13$. However, judging from the other large E2 matrix elements obtained in this study, at least the lower parts of the band are strongly disturbed. This can be interpreted as a mixing of different modes of excitation.

The exceptionally intense $0_3^+ \rightarrow 0_2^+$ transition can be interpreted in the framework of deformation and configuration mixing: in producing a large ρ^2 value one would need a strong mixing of components with different shapes in the wave functions of the 0_2^+ and 0_3^+ states. Explicitly, a component associated with the same deformation in both of the wave functions produces a nonzero monopole matrix element. This kind of mixing is reasonable because of the small energy difference of the 0_2^+ and 0_3^+ levels. For example, if completely mixed spherical and deformed states are assumed i.e.

$$|\,0_3^+\rangle = \frac{1}{\sqrt{2}}\,|\,\mathrm{sph}\rangle - \frac{1}{\sqrt{2}}\,|\,\mathrm{def}\rangle\ ,$$

$$|\,0_2^+\rangle = \frac{1}{\sqrt{2}}\,|\,\mathrm{sph}\rangle + \frac{1}{\sqrt{2}}\,|\,\mathrm{def}\rangle\ ,$$

a monopole matrix element

$$m(E0) = \langle 0_2^+ \mid \sum_i e\, r_i^2 \mid 0_3^+ \rangle = \frac{1}{2}\, k\, \beta^2,$$

where k is a parameter defined by Bohr and Mottelson[68], is obtained. This gives

$$\rho = \frac{m(E0)}{eR^2} = 6.8\, \beta^2 ,$$

which requires a value of $\beta = 0.22$ for the deformation parameter in order to yield the experimental value of $\rho^2 = 100 \times 10^{-3}$ in ^{116}Sn. If the mixing is less strong, then β would have to be still larger. Of course, no quantitative calculation can be made with this crude model.

A considerable difference between the E2 decay rates of the 0_2^+ and 0_3^+ states to the 2_1^+ state indicates differences in the nondeformed parts of the mixed wave functions of these 0^+ states: the 0_2^+ state seems to contain a two-phonon component, while the sensitivity of the $X(0_3^+ \rightarrow 0_1^+)$ value to the neutron number indicates that neutron particle excitations play an important role in the 0_3^+ states.

A possible explanation for the changes of the present E2 and E0 transition rates in going to ^{114}Sn could be the $g_{7/2} + d_{5/2}$ subshell closure. Relatively strong transitions to the 0_2^+ and 0_3^+ states of ^{114}Sn in the (t,p) reaction are interpreted as an effect of this subshell closure, which carries the description of the 0^+ states closer to the neutron pairing-vibrational picture[50].

5. DECAY OF 0_2^+ AND 0_3^+ STATES IN ^{112}Cd and ^{114}Cd

5.1. Introduction

The picture of the spherical vibrational even mass Cd nuclei was disturbed by the observation of a sizeable static quadrupole moment of the 2_1^+ state in these nuclei. Furthermore, it is well known that the ^{112}Cd and ^{114}Cd nuclei exhibit "extra" 0_3^+ and 2_3^+ levels among the 0_2^+, 2_2^+ and 4_1^+ levels of the two-phonon triplet. These states can be associated with a second minimum of a collective potential energy surface calculated in ref.72. Consequently, the 0_3^+ and 2_3^+ states are proposed as members of a rotational band built on the deformed 0_3^+ state. However, problems arise from the identification of the other band members.

In a recent (^{3}He,n) study[47] a strong L=0 transition to the 0_2^+ state in ^{110}Cd and ^{112}Cd was observed. This would indicate a similarity of the 0_2^+ states in even Cd nuclei to those in Sn, i.e. proton excitations play an important role in these states. On the basis of this result the above-mentioned deformation could be associated with the 0_2^+ state as in Sn. Recently quasirotational bands built on the 0_2^+ states in ^{110}Cd and ^{114}Cd have been proposed in ref.73.

The E0 and E2 decay properties of the 0_2^+ and 0_3^+ states in ^{114}Cd have been measured previously [74-77] utilizing the enormous cross section of the ^{113}Cd(n,γ)^{114}Cd reaction. In ^{112}Cd only the E2($0_3^+ \rightarrow 2_2^+$)/E2($0_3^+ \rightarrow 2_1^+$) ratio has been reported previously from ^{112}Ag decay[78,79].

5.2. Measurements and results

In the present work the intermediate-image magnetic plus Si(Li) electron spectrometer described in subsect. 2.2.1 in different modes of operation was employed.

The E0/E2 branching ratio of the 0_2^+ state in ^{112}Cd was obtained from the singles electron and γ-ray spectra following the β^+ decay of 14.4 min ^{112}In. This activity was produced in bombardments of an enriched metallic ^{112}Cd foil of about 1 mg/cm^2 thickness with 11 MeV protons from the cyclotron in runs of 20 min length. The resulting value for the K conversion electrons is $I_K(E0;\ 0_2^+ \rightarrow 0_1^+)/I_K(E2;\ 0_2^+ \rightarrow 2_1^+) = 0.33 \pm 0.05$.

The 0_3^+ state was excited in the ^{111}Cd(d,p)^{112}Cd reaction. An enriched metallic ^{111}Cd foil of 0.8 mg/cm^2 thickness and a beam of 9 MeV deuterons from the cyclotron were used in this investigation. The 0_3^+ state in ^{112}Cd is de-excited by two E0 and two E2 transitions. The resolving and confirmation of the low-energy $0_3^+ \rightarrow 0_2^+$ and $0_3^+ \rightarrow 2_2^+$ transitions in the complex part of the electron and γ-ray spectra are possible only with the aid of e^-p and γp coincidence measurements. A γp coincidence arrangement with an Al absorber in front of a thin surface-barrier detector described in sect. 2.1 was employed. In the e^-p coincidence experiment the electron - heavy-particle coincidence set-up, with a 0.5 mm thick Al absorber in front of the annular particle detector, was successfully applied. This experiment is described in subsect. 2.2.2 and the resulting coincidence spectrum is illustrated in fig. 16. This figure shows, among several drastic differences

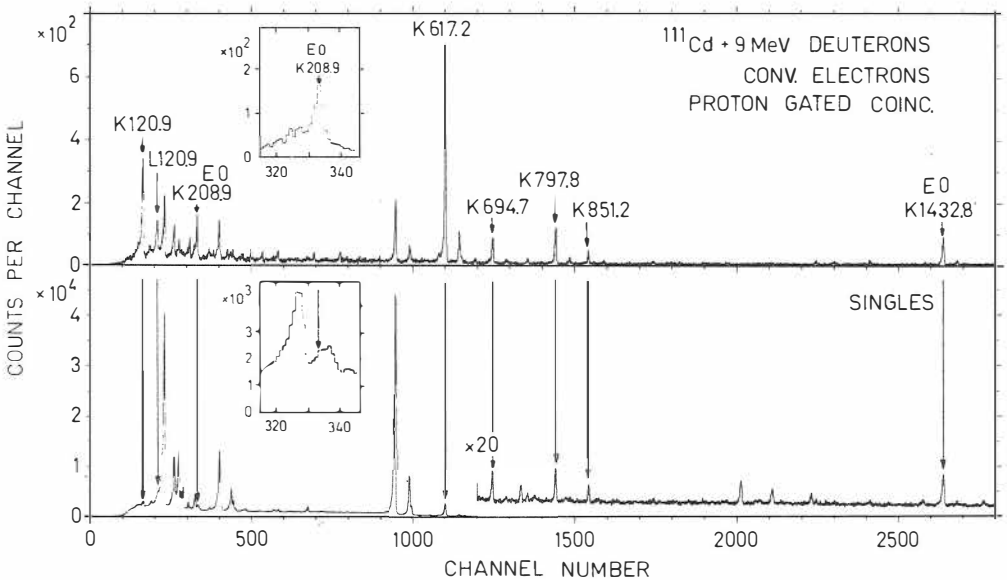

Fig. 16. Conversion-electron spectra obtained by bombarding a ^{111}Cd target of 0.8 mg/cm^2 thickness with 9 MeV deuterons. Some of the lines belonging to the (d,p) reaction are indicated with arrows.

between the singles and coincidence spectra, how a line corresponding to the $E0(0_3^+ \rightarrow 0_2^+)$ transition in ^{112}Cd masked by a very complex part of the direct electron spectrum is clearly resolved in the coincidence spectrum.

From these coincidence and several singles γ-ray and electron spectra, branching ratios for the decay of the 0_3^+ state in ^{112}Cd can be derived. The result expressed as K conversion-electron intensities is: $I_K(E0;\ 0_3^+ \rightarrow 0_1^+)/I_K(E2;\ 0_3^+ \rightarrow 2_1^+)/I_K(E0;\ 0_3^+ \rightarrow 0_2^+)/I_K(E2;\ 0_3^+ \rightarrow 2_2^+)$= 0.79(8)/0.10(3)/2.5(4)/11(2). The observed ratio $I_\gamma(E2;\ 0_3^+ \rightarrow 2_2^+)/I_\gamma(E2;\ 0_3^+ \rightarrow 2_1^+)$ = 0.3 is in disagreement with the value of 1.7 reported in ref.78 but is closer to the value of 0.6 in ref. 79.

The high-efficiency coincidence method was employed in the double Coulomb excitation measurements, in which thick (15 mg/cm^2) metallic Cd targets were bombarded with a 44 MeV ^{16}O beam from the Tandem. Preliminary values of reduced $E2(0_2^+ \rightarrow 2_1^+)$ transition probabilities determined from these measurements are 51±13 W.u. ($T_{1/2}(0_2^+)$= 4.2 ps) in ^{112}Cd and 41±8 W.u. ($T_{1/2}(0_2^+)$ = 6.6 ps) in ^{114}Cd. The latter value is 35 % higher than that of ref. 77.

The intermediate-image magnetic plus Si(Li) electron spectrometer, in conjunction with the pulsed beam of the cyclotron, was used to determine the half-lives of the 0_3^+ states in ^{112}Cd and ^{114}Cd. This arrangement and the measurement in the ^{112}Cd case are described in subsect. 2.3.3 , where a half-life value of 1.9±0.1 ns was derived. In the ^{114}Cd case the $^{113}Cd(d,p)^{114}Cd$ reaction was used to populate the 0_3^+ level by bombarding an enriched ^{113}Cd metallic foil of 0.7 mg/cm^2 thickness with 8 MeV deuterons from the cyclotron. Results of this two-parameter run are shown in fig. 17, where the prompt shape

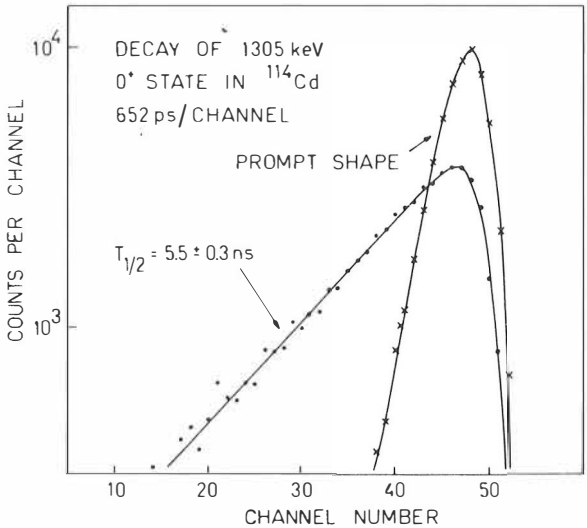

Fig. 17. Half-life measurement of the 1305 keV 0_3^+ state in ^{114}Cd

corresponds to the conversion electrons of the 558 keV $2_1^+ \rightarrow 0_1^+$ transition. The half-life value for the 0_3^+ state in ^{114}Cd directly derived from the slope of the time-delay distribution is 5.5±0.3 ns, which is the same as that of ref.76, where a $\gamma\gamma$ coincidence arrangement in conjunction with the (n,γ) reaction was employed.

A summary of the present experimental results is shown in fig. 18. In table 3 the transition energies, X values and reduced transition probabilities are tabulated. In the ^{114}Cd case the γ-ray and conversion-electron intensities of refs.74,75 are used in the calculations.

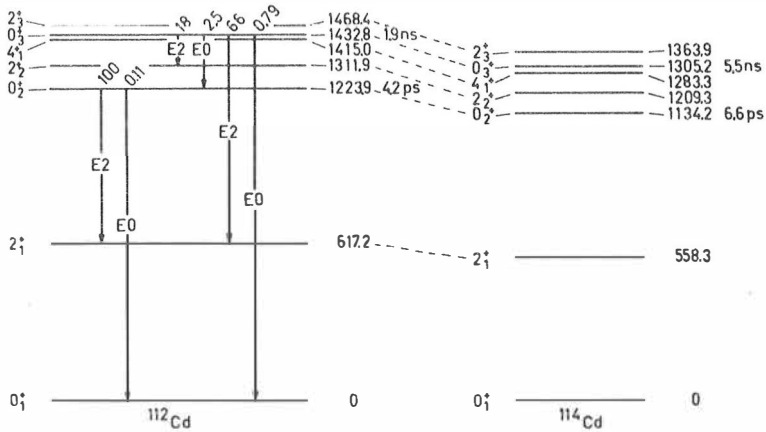

Fig. 18. Partial level schemes of ^{112}Cd and ^{114}Cd. Half-lives and transition intensities determined in this work are included. The E0 and E2 intensities are K conversion-electron and γ-ray intensities, respectively. Level energies of ^{112}Cd and ^{114}Cd are from this work and ref.80, respectively.

5.3. Discussion

The decays of the 0_2^+ and 0_3^+ states in ^{112}Cd and ^{114}Cd are roughly in accordance with the naive spherical vibrator model if these states are interpreted as a two-phonon and a three-phonon state, respectively: the E2($0_2^+ \rightarrow 2_1^+$) and E2($0_3^+ \rightarrow 2_2^+$) transitions are enhanced, the

Table 3. Data on ^{112}Cd and ^{114}Cd

	^{112}Cd	^{114}Cd a)		^{112}Cd	^{114}Cd
$E0(0_2^+\to0_1^+)$(keV)	1223.9	1134.2	$\frac{B(E2;0_2^+\to2_1^+)}{B(E2)_{W.u.}}$	51(13)	41(8)
$E2(0_2^+\to2_1^+)$(keV)	606.7	575.9	$T_{1/2}(0_2^+)$(ps)	4.2(10)	6.6(12)
$X\left(\frac{E0;0_2^+\to0_1^+}{E2;0_2^+\to2_1^+}\right)$	0.026(4) b)	0.026(5) b)	$\rho^2(0_2^+\to0_1^+)\cdot10^3$	37(11) b)	30(8) b)
			$\rho^2(0_2^+\to0_1^+)$	0.19(3)	0.17(2)
$E0(0_3^+\to0_1^+)$(keV)	1432.8	1305.2	$\frac{B(E2;0_3^+\to2_1^+)}{B(E2)_{W.u.}}$	0.017(4)	0.0038(5)
$E2(0_3^+\to2_1^+)$(keV)	815.6	746.9	$\frac{B(E2;0_3^+\to2_2^+)}{B(E2)_{W.u.}}$	66(20)	101(7)
$E0(0_3^+\to0_2^+)$(keV)	208.9	171.0	$T_{1/2}(0_3^+)$(ns)	1.9(1)	5.5(3)
$E2(0_3^+\to2_2^+)$(keV)	120.9	95.9	$\rho^2(0_3^+\to0_1^+)\cdot10^3$	0.48(11)	1.7(2)
$X\left(\frac{E0;0_3^+\to0_1^+}{E2;0_3^+\to2_1^+}\right)$	1.0(2)	16(3)	$\rho^2(0_3^+\to0_2^+)\cdot10^3$	8.1(19)	0.41(9)
$X\left(\frac{E0;0_3^+\to0_2^+}{E2;0_3^+\to2_1^+}\right)$	17(4)	3.8(9)	$\rho(0_3^+\to0_1^+)$	0.022(3)	0.042(3)
$X\left(\frac{E0;0_3^+\to0_1^+}{E2;0_3^+\to2_2^+}\right)\cdot10^4$	2.6(6)	6.0(6)	$\rho(0_3^+\to0_2^+)$	0.090(11)	0.020(2)
$X\left(\frac{E0;0_3^+\to0_2^+}{E2;0_3^+\to2_2^+}\right)\cdot10^4$	43(11)	1.41(14)			

a) Energies from ref.80, $I_\gamma(E2;0_3^+\to2_1^+)/I_\gamma(E2;0_3^+\to2_2^+)$ from ref.74 and E0 transition intensities from ref.75.

b) Spherical-vibrator values[66,67]: $X=0.035$, $\rho^2=63\times10^{-3}$ for ^{112}Cd and $X=0.037$, $\rho^2=73\times10^{-3}$ for ^{114}Cd.

$E0(0_2^+ \rightarrow 0_1^+)$ transition is relatively strong, the $E2(0_3^+ \rightarrow 2_1^+)$ transition is very hindered and the other E0 transitions are weak. However, the assumed three-phonon 0_3^+ state is strongly pushed down in energy, which could be explained as being due to γ softness[73].

The intriguing question in even mass Cd nuclei is the possible deformation associated with either the 0_2^+ or the 0_3^+ state. Usually the 0_3^+ state is supposed to belong to the second minimum of the potential energy surface. However in ref.73 the 0_2^+ state is identified with a deformed band head in ^{114}Cd, the deformation being generated by proton excitations in this state. This assumption is supported by the recent (^{3}He,n) results[47]. The present results, especially the strong E2 transitions from the 0_2^+ and the 0_3^+ states in ^{112}Cd and ^{114}Cd, indicate the presence of collective components in the wave functions of these states. The E0 transition rate between these excited 0^+ states is much weaker than that in the even Sn nuclei. According to the crude model used for the Sn nuclei, one may say that a mixing of different shapes in the wave functions of the 0_2^+ and 0_3^+ states is not as strong as in the Sn nuclei or the deformation associated with these states is weaker. In this respect, the situation in ^{112}Cd is much closer to the Sn case since the $\rho^2(0_3^+ \rightarrow 0_2^+)/\rho^2(0_3^+ \rightarrow 0_1^+) = 17$.

Concerning the systematics of the low-lying 0^+ states in the even Cd nuclei, it would be interesting to study other Cd isotopes. Preliminary results of the present investigation show that in ^{110}Cd the 0_3^+ level cannot be found among the two-phonon triplet and in ^{116}Cd the collective 0_2^+ level is well above the other two-phonon levels.

6. SUMMARY

The present results show that the development of suitable in-beam electron spectrometer arrangements and lifetime measurement methods, and the use of ion beams from a small cyclotron and a Tandem Van de Graaff accelerator have rendered it possible to obtain systematic data on the decay of low-lying 0^+ states in even mass nuclei.

The half-lives of the 0_2^+ states in ^{206}Pb and ^{208}Po were determined by means of a magnetic lens plus fast plastic scintillation detector set-up utilizing very short micropulses from the Jyväskylä cyclotron. The earlier confusion associated with the decay properties of the 0_2^+ state in ^{208}Po was cleared up. The E0 and E2 transitions from the 0_2^+ states in ^{206}Pb and ^{208}Po were shown to be similar, which indicates that both of these states are fairly pure two-neutron-hole states. The use of the experimental isotope-shift data in producing the observed E0 transition probability in ^{206}Pb was shown to be meaningless because of the incompleteness of these data.

The first extensive systematic investigation of the decay properties of the 0^+ states was carried out in even $^{112-120}$Sn nuclei. In this investigation, various magnetic lens plus Si(Li) electron spectrometers were employed. A high-efficiency intermediate-image magnetic plus Si(Li) electron spectrometer in conjunction with an annular particle detector was used in resolving the low-energy E0 transitions between the excited 0^+ states in $^{114-120}$Sn. A high-efficiency coincidence method for double Coulomb excitation measurements was an important

method in determining the transition rates from the collective 0_2^+ states. A walk-free centroid method was developed to obtain the results of the half-lives of the 0_2^+ and 0_3^+ states in ^{116}Sn and the 0_3^+ state in ^{118}Sn.

The intermediate-image magnetic plus Si(Li) electron spectrometer in singles, direct lifetime measurement and e^-p coincidence modes of operation was successfully applied in determining the decay properties of the 0_2^+ and 0_3^+ states in ^{112}Cd and ^{114}Cd.

The present results on the Sn and Cd nuclei show that the wave functions of the 0_2^+ states in these nuclei contain strong collective components. The intense E0 transition between the excited 0^+ states in Sn nuclei indicates that these states are mixed and that deformation probably is associated with both of these states. On the other hand, in ^{112}Cd and ^{114}Cd, the $0_3^+ \rightarrow 0_2^+$ transition is not as strong, which implies a weaker mixing or weaker deformation.

It is evident that more complicated theoeretical models are called for to explain the decay properties of the 0_2^+ and 0_3^+ states in the even Sn and Cd nuclei. The present systematic data could be of great value in this theoretical work. It would be particularly interesting to know the real nature of the 0_2^+ level, which exhibits characteristics of a phonon, deformed and proton pairing-vibrational state. Since an E0 transition is some kind of a measure of mixing and deformation, the role of low-energy E0 transitions between the excited 0^+ states is important in the study of the decay properties of 0^+ states.

References

1) N. A. Voinova, The 0^+ states and electric monopole transitions in even-even atomic nuclei, INDC (CCP)-93/N, IAEA, Vienna, 1976

2) E. L. Church and J. Weneser, Phys. Rev. 103 (1956) 1035

3) J. O. Rasmussen, Proc. Nucl. Structure Symp., Dubna 1968, IAEA STI/PUB 189, p. 169

4) S. V. Kamerdzhiev, Sov. J. Nucl. Phys. 11 (1970) 301

5) B. F. Bayman, A. S. Reiner and R. K. Sheline, Phys. Rev. 115 (1959) 1627

6) D. R. Bès and R. A. Broglia, Nucl. Phys. 80 (1966) 289

7) E. R. Flynn and P. D. Kunz, Phys. Lett. 68B (1977) 40

8) A. S. Davydov, Nucl. Phys. 24 (1961) 682

9) R. A. Meyer, R. D. Griffioen, J. Graber Lefler and W. B. Walters, Phys. Rev. C 14 (1976) 2024

10) J. Kantele, M. Luontama, A. Passoja and R. Julin, Nucl. Instr. and Meth. 130 (1975) 467

11) M. Luontama, J. Kantele, R. Julin, A. Passoja, T. Poikolainen and M. Pylvänäinen, Nucl. Instr. and Meth., 159 (1979) 339

12) R. Julin, J. Kantele, M. Luontama, T. Poikolainen and V. Rahkonen, Phys. Lett. 65B (1976) 337

13) R. Julin, J. Kantele, M. Luontama, A. Passoja and T. Poikolainen, Nucl. Instr. and Meth. 152 (1978) 471

14) L. Westerberg, L. O. Edvardson, G. Ch. Madueme and J. E. Thun, Nucl. Instr. and Meth. 128 (1975) 61

15) M. J. Canty, P. H. Debenham, D. A. Dohan, M. Skalsey and J. W. Watson, Nucl. Instr. and Meth. 122 (1974) 547

16) W. D. Schneider and K. H. Gonsior Nucl. Instr. and Meth. 130 (1975) 165

17) P. Kleinheinz, L. Samuelsson, R. Vukanović and K. Sieghahn, Nucl. Instr. and Meth. 32 (1965) 1

18) H. J. Kim and W.T. Milner, Nucl. Instr. and Meth. 95 (1971) 429

19) D. C. S. White, W. J. McDonald, D. A. Hutcheon and G. C. Neilson, Nucl. Phys. A260 (1976) 189

20) J. Lindskog and Lars-Göran Svensson, Nucl. Instr. and Meth. 133 (1976) 99

21) D. B. Fossan and E. K. Warburton, in Nuclear spectroscopy and reactions, ed. J. Cerny (Academic Press, New York, 1974) part C, ch. VII H.

22) P. Salling, Phys. Lett. 17 (1965) 139

23) O. Häusser, F. C. Khanna and D. Ward, Nucl. Phys. A194 (1972) 113

24) T. D. Newton, Phys. Rev. 78 (1950) 490

25) D. A. Hutcheon, Nucl. Instr. and Meth. 113 (1973) 221

26) E. de Lima, H. Kawakani, A. de Lima, R. Hichwa, A. V. Ramayya, J. H. Hamilton and W. Dunn, Nucl. Instr. and Meth. 151 (1978) 221

27) N.-G. Jonsson, J. Kantele and A. Bäcklin,
Nucl. Instr. and Meth. 152 (1978) 485

28) A. Winther and J. de Boer, Coulomb excitation, eds. K. Alder and
A. Winther (Academic Press, New York, 1966)

29) W. W. True, Phys. Rev. 168 (1968) 1388

30) E. R. Flynn, G. J. Igo, R. Woods, P. D. Barnes and N. K. Glendenning,
Phys. Rev. Lett. 19 (1967) 798

31) V. Rahkonen, E. Liukkonen, J. Hattula, P. Kettunen and J. Muhonen
Annual Report of JYFL 1976, Jyväskylä, unpublished

32) T. S. Bhatia, T. R. Canada, P. D. Barnes, R. Eisenstein, C. Ellegaard
and E. Romberg, Phys. Rev. Lett. 30 (1973) 496

33) H. C. Griffin and A. M. Donne, Phys. Rev. Lett. 28 (1972) 107

34) J. W. Tape, E. G. Adelberger, D. Burch and L. Zamick,
Phys. Rev. Lett. 29 (1972) 878

35) L. H. Goldman, B. L. Cohen, R. A. Moyer and R. C. Diehl,
Phys. Rev. C 1 (1970) 1781

36) P. Richard, N. Stein, C. D. Kavaloski and J. S. Lilley,
Phys. Rev. 171 (1968) 1308

37) R. S. Hager and E. C. Seltzer, Nucl Data A6 (1969) 1

38) V. P. Krainov and M. A. Mikulinskii,
Sov. J. Nucl. Phys. 4 (1967) 665

39) R. Engfer, H.Schneuwly, J. L. Vuilleumier, H. K. Walter and A. Zehnder,
Atomic Data and Nuclear Data Tables 14 (1974) 509

40) J. Speth, L. Zamick and P. Ring, Nucl. Phys. A232 (1974) 1

41) C. W. Ma and W. W. True, Phys. Rev. C 8 (1973) 2313

42) Reviews are given by E. U. Baranger, in Advances in nuclear physics vol. 4, ed. by M. Baranger and E. Vogt (Plenum Press, New York, 1971); O. Beer, A. El Behay, P. Lopato, Y. Terrie , C. Vallois, K. K. Seth, Nucl. Phys. A147 (1970) 326

43) R. Raj, Y. K. Gambhir and M. K. Pal, Phys. Rev. 163 (1967) 1004

44) W. F. van Gunsteren, K. Allaart and E. Boeker, Z. Physik 267 (1974) 87;
W. F. van Gunsteren and K. Allaart, Z. Physik A276 (1976) 1

45) G. Bonsignori and M. Savoia, Istituto di Fisica dell' Universita di Bologna, Italy, preprint (1977)

46) D. M. Clement and E. U. Baranger, Nucl. Phys. A120 (1968) 25

47) H. W. Fielding, R.E. Anderson, C. D. Zafiratos, D. A. Lind, F. E. Cecil, H. H. Wieman and W. P. Alford, Nucl. Phys. A281 (1977) 389

48) J. Bron, W. H. A. Hesselink, L. K. Peker, A. van Poelgeest, J. Vitzinger, H. Verheul, J. Zalmstra, Proc. Int. Conf. Nucl. Structure, Contributed papers, Tokyo, Sept. 5-10, 1977 (International Academic Printing Co., Ltd., Tokyo, 1977)

49) E. J. Schneid, A. Prakash and B. L. Cohen, Phys. Rev. 156 (1967) 1316

50) J. H. Bjerregaard, O. Hansen and O. Nathan, Nucl. Phys. A131 (1969) 481

51) T. Yamazaki and G. T. Ewan, Nucl. Phys. A134 (1969) 81

52) D. G. Fleming, M. Blann, H. W. Fulbright and J. A. Robbins, Nucl. Phys. A157 (1970) 1

53) F. Pleiter, Nucl. Phys. A184 (1972) 443

54) Y. Yamaguchi, J. Ruan (Gen) and T. Nagahara, J. Phys. Soc. Japan 38 (1975) 911

55) H. Kawakami et al., Annual Report of INS 1974, Tokyo, unpublished

56) P. Richard, C. F. Moore, J. A. Becker and J. D. Fox, Phys. Rev. 145 (1966) 971

57) A. Bäcklin, W. Dietrich, R. Julin, J. Kantele, M. Luontama and L. Westerberg, Phys. Lett. 62B (1976) 402

58) A. Bäcklin, N.-G. Jonsson, R. Julin, J. Kantele, M. Luontama, A. Passoja and T. Poikolainen, to be published

59) E. J. Schneid, E. W. Hamburger and B. L. Cohen, Phys. Rev. 161 (1967) 1208

60) J. Kantele, R. Julin, M. Luontama, A. Passoja, T. Poikolainen, A. Bäcklin and N.-G. Jonsson, Z. Physik A289 (1979) 157

61) D. Rabenstein, Z. Physik 240 (1970) 244

62) G. H. Carlson, W. L. Talbert and S. Raman, Nuclear Data Sheets 14 (1975) 247

63) G. H. Carlson, W. L. Talbert and S. Raman, Nuclear Data Sheets 17 (1976) 1

64) A. V. Aldushchenkov and N. A. Voinova, Nuclear Data Tables 11 (1972) 299

65) R. S. Hager and E. C. Seltzer, Nucl. Data A4 (1968) 1

66) H. Kumar, in The electromagnetic interaction in nuclear spectroscopy, ed. W. D. Hamilton (North-Holland, Amsterdam, 1975) ch.3

67) P. H. Stelson and L. Grodzins, Nucl. Data A1 (1965) 21

68) A. Bohr and B. Mottelson, Nuclear structure, vol.2 (W. A. Benjamin, New York, 1975)

69) S. V. Jackson and R. A. Meyer, Phys. Rev. C 15 (1977) 1806

70) J. Ludziejewski, private communication;
B. Nerlo-Pomorska and J. Ludziejewski, Z. Physik A287 (1978) 337

71) K. Heyde, private communication

72) G. Gneuss and W. Greiner, Nucl. Phys. A171 (1971) 449

73) R. A. Meyer and L. Peker, Z. Physik A283 (1977) 379

74) L. V. Groshev, A. M. Demidov, V. I. Pelekhov, L. L. Sokolovskii, G. A. Bartholomev, A. Doveika, K. M. Eastwood and S. Monaro, Nucl. Data A5 (1968) 1

75) A. Bäcklin, N. E. Holmberg and G. Bäckström, Nucl. Phys. 80 (1966) 154

76) B. Fogelberg, A. Bäcklin and J. McDonald, Fizika 7 (1975) 218

77) F. K. McGowan, R. L. Robinson, P. H. Stelson and J. L. C. Ford, Jr., Nucl. Phys. 66 (1965) 97

78) J. A. Macdonald and H. D. Sharma, Nucl. Phys. A156 (1970) 321

79) G. Wallace, G. J. McCallum and N. G. Chapman, Nucl. Phys. A182 (1972) 417

80) H. J. Kim, Nuclear Data Sheets 16 (1975) 107